Rapid and strain-specific resistance evolution of *Staphylococcus aureus* against inhibitory molecules secreted by *Pseudomonas aeruginosa*

Selina Niggli[1*], Lucy Poveda[2], Jonas Grossmann[2], Rolf Kümmerli[1**]

[1] Department of Quantitative Biomedicine, University of Zurich, Winterthurerstrasse 190, 8057 Zurich, Switzerland

[2] Functional Genomics Center Zurich, ETH Zurich and University of Zurich, Winterthurerstrasse 190, 8057 Zurich, Switzerland

Corresponding authors:

* selina.niggli@uzh.ch

** rolf.kuemmerli@uzh.ch

Abstract

Pseudomonas aeruginosa and *Staphylococcus aureus* frequently occur together in polymicrobial infections, and there is evidence that their interactions negatively affect disease outcome in patients. At the molecular level, interactions between the two bacterial taxa are well-described, with *P. aeruginosa* usually being the dominant species suppressing *S. aureus* through a variety of inhibitory molecules. However, in polymicrobial infections, the two species interact over prolonged periods of time, and *S. aureus* might evolve resistance against inhibitory molecules deployed by *P. aeruginosa*. Here, we used experimental evolution to test this hypothesis by exposing three different *S. aureus* strains (Cowan I, 6850, JE2) to the growth-inhibitory supernatant of *P. aeruginosa* PAO1 over 30 days. We found that all three *S. aureus* strains rapidly evolved resistance against inhibitory molecules and show that (i) adaptations were strain-specific; (ii) resistance evolution affected the expression of virulence traits; and (iii) mutations in membrane transporters were the most frequent evolutionary targets. Our work indicates that adaptations of *S. aureus* to co-infecting pathogens could increase virulence and decrease antibiotic susceptibility, because both virulence traits and membrane transporters involved in drug resistance were under selection. Thus, pathogen co-evolution could exacerbate infections and compromise treatment options.

Introduction

Bacterial infections are frequently caused by multiple species (Brogden, Guthmiller, and Taylor 2005; Peters et al. 2012) and such polymicrobial infections can be more severe than the respective mono-species infections (Jorge et al. 2018; Lim, Lim, and Ray 2013; Pammi et al. 2014; Tan et al. 2016). Because of the detrimental effects for patients, there is high interest in understanding the mechanisms of bacterial interactions and how they affect ecological dynamics between co-infecting species. Interactions between the two opportunistic human pathogens *Pseudomonas aeruginosa* (PA) and *Staphylococcus aureus* (SA) have attracted particularly high attention (Hotterbeekx et al. 2017; Limoli and Hoffman 2019). This is because they are major pathogens and often co-occur in the lungs of cystic fibrosis (CF) patients, and in burn and chronic wound infections (Dowd et al. 2008; Gjødsbøl et al. 2006; Hubert et al. 2013; Maliniak, Stecenko, and McCarty 2016). Co-infections with PA and SA can be associated with more severe disease outcomes in humans (Gangell et al. 2011; Maliniak, Stecenko, and McCarty 2016), and studies in animal models confirmed increased virulence and compromised antibiotic treatment options during co-infections (Dalton et al. 2011; Hendricks et al. 2001; Pastar et al. 2013).

Laboratory studies established a solid mechanistic understanding of how the two species interact, and generally agree that the relationship between PA and SA is antagonistic (Filkins et al. 2015; Niggli and Kümmerli 2020; Yung, Sircombe, and Pletzer 2021). Overall, PA seems to dominate the interactions through the production and secretion of a variety of inhibitory molecules, such as the staphylolytic protease LasA, siderophores, and the respiratory chain inhibitors HQNO and phenazines (Harrison et al. 2008; Hoffman et al. 2006; Kessler et al. 1993; Lin et al. 2018; Mashburn et al. 2005; Soberón-Chávez, Lépine, and Déziel 2005). There is also increasing knowledge on ecological factors that influence interactions patterns. For example, during early childhood, CF lungs are often first colonized by SA followed by PA later on, with SA abundance tending to decrease when PA increases (Nguyen and Oglesby-Sherrouse 2016). In the context of wound infections, we also have an increased

58 understanding about the spatial localization of the two species, where it seems that PA and
59 SA occupy different niches (Fazli et al. 2009; Phalak et al. 2016).

60 In contrast to these mechanistic and ecological insights, we know little about whether
61 interactions between PA and SA can evolve. Species co-evolution is likely to occur in chronic
62 infections, where pathogens repeatedly interact, and is predicted to alter disease parameters
63 and treatment strategies. In the context of interactions between PA and SA, we hypothesize
64 that SA could adapt and become resistant to PA inhibitory molecules. Such adaptation could
65 in turn foster co-existence of the two species, potentially contribute to the clinically observed
66 higher virulence, increased morbidity and treatment complications (Gangell et al. 2011;
67 Maliniak, Stecenko, and McCarty 2016).

68 Here, we test our hypothesis by using a combination of experimental evolution,
69 phenotypic screening, and whole-genome sequencing of evolved clones. Specifically, we first
70 conducted a series of experiments with three different clinical SA strains to show that all of
71 them are inhibited by a secreted compound regulated by the PQS quorum-sensing system in
72 the supernatant of the PA standard laboratory strain PAO1. We then exposed the three SA
73 strains to either the PA supernatant (containing inhibitory molecules, mixed with fresh medium)
74 or regular medium only (as a control) for 30 consecutive days, by transferring evolving cultures
75 every 48 hours to fresh PA supernatant or regular medium. Following experimental evolution,
76 we isolated evolved SA clones from replicated populations to screen them for resistance
77 phenotypes and to explore whether virulence traits were under selection. Finally, we
78 sequenced the whole genome of 150 clones to determine the genetic basis of SA resistance
79 evolution against inhibitory molecules produced by PA.

80

81 **Results**

82 **Growth of SA strains is reduced in the presence of PA supernatant**

83 Previous work showed that PA can inhibit SA via a diverse set of secreted molecules, including
84 proteases, biosurfactants, siderophores, and toxic compounds (Hotterbeekx et al. 2017). To
85 test whether our three SA strains (Cowan I, 6850 and JE2, Table S1) are also inhibited by PA,

we exposed them to the sterile-filtered supernatant of PA PAO1, harvested from overnight cultures (30% supernatant in 70% fresh tryptic soy broth, TSB). We found that all three SA strains were negatively affected by the PA supernatant compared to growth under control condition (30% NaCl in 70% TSB, Figure 1). Exposure to PA supernatant significantly reduced overall growth performance (Figure S1a, ANOVA on growth integrals followed by Tukey's HSD pairwise comparisons: $p_{adj} < 0.0001$ for all SA strains), and specifically extended the lag phase of all SA strains (Figure S1b). We also observed SA strain-specific responses (Figure 1). Cowan I featured an intermediate extension of the lag phase (10.3 hours compared to 6.6 hours in the control medium), a premature stationary phase, followed by a decrease in OD_{600} possibly indicating cell death. 6850 suffered from an extremely long lag phase extension (19.7 hours vs. 6.9 hours), also showed a premature growth stop, but no OD_{600} decline. JE2 was least affected by the PA supernatant. Its lag phase extension was not as pronounced (8.4 hours vs. 5.6 hours), and it grew steadily afterwards, albeit to a lower yield than the control.

We also conducted the reciprocal experiments by exposing PA to the supernatants of the three SA strains, but found no inhibition (Figure S2). Taken together, our supernatant assays reveal unilateral inhibition: PA produces inhibitory molecules that negatively affect the growth of genetically different SA strains.

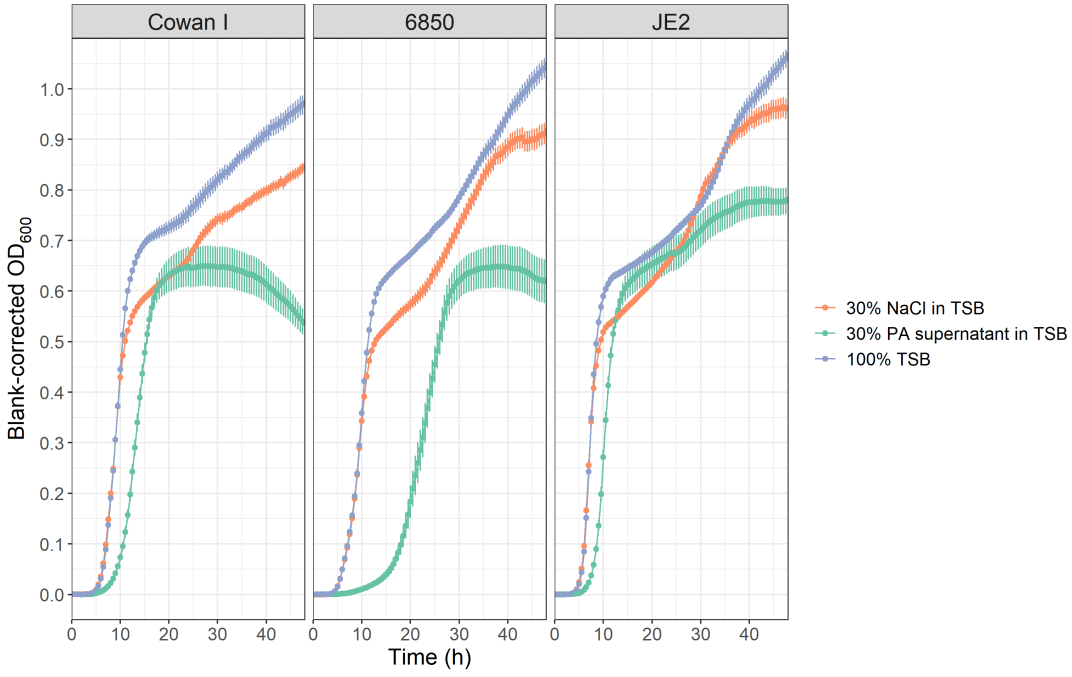

Figure 1. Supernatant of PA inhibits growth of three different SA strains (Cowan I, 6850, JE2). Growth trajectories of SA strains were followed over 48 hours at 37 °C under three different conditions: 30% NaCl in TSB (control 1), 30% PA supernatant in TSB (experimental treatment) and 100% TSB (control 2). Curves show the average growth (± standard error) across seven independent experiments and a total of 28 replicates per strain and condition. See Figure S1 for a statistical comparison of growth parameters extracted from these curves.

The PQS pathway is involved in compromising SA growth

To identify possible PA pathways or traits involved in the inhibition of SA, we screened a small panel of seven PA candidate mutants and checked whether the inhibitory effects of their supernatants towards SA were altered. We found one hit: the supernatant of PAO1*ΔpqsA* did no longer inhibit SA (Table 1, Figure S3).

Table 1. Relative effects of supernatants from wildtype and mutant *P. aeruginosa* (PA) strains on *S. aureus* (SA) growth.

PA supernatant donor strain	Phenotype of mutant strain	Relative growth* of Cowan I in PA supernatant	Relative growth* of 6850 in PA supernatant	Relative growth* of JE2 in PA supernatant
PAO1 wild type	wild type	0.78 (± 0.20)	0.60 (± 0.23)	0.87 (± 0.18)
MPAO1 wild type	wild type	0.75 (± 0.23)	0.59 (± 0.21)	0.72 (± 0.18)
PAO1*ΔlasR*	Las quorum sensing signal blind	0.34 (± 0.08)	0.38 (± 0.10)	0.50 (± 0.19)
PAO1*ΔrhlI*	Rhl quorum sensing signal negative	0.65 (± 0.05)	0.45 (± 0.11)	0.67 (± 0.05)
PAO1*ΔrhlR*	Rhl quorum sensing signal blind	0.70 (± 0.13)	0.60 (± 0.05)	0.70 (± 0.03)
PAO1*ΔrhlA*	Rhamnolipid null mutant	0.61 (± 0.11)	0.54 (± 0.15)	0.68 (± 0.07)
MPAO1*ΔpqsA*	Alkylquinolone null mutant	**1.22 (± 0.16)**	**1.22 (± 0.10)**	**1.05 (± 0.12)**
PAO1*ΔpvdDΔpchEF*	Siderophore null mutant	0.63 (± 0.01)	0.23 (± 0.04)	0.68 (± 0.02)
PAO1*ΔlecA*	Lectin null mutant	0.67 (± 0.02)	0.42 (± 0.01)	0.83 (± 0.06)

*The relative supernatant effect (± standard deviation) is expressed as the growth integral of SA over 48 hours in 30% PA supernatant + TSB divided by the growth integral of SA in 30% NaCl + TSB. Values < 1 indicate growth inhibition, while values > 1 (in bold) indicate cases with no inhibition.

PqsA is an anthranilate-coenzyme A ligase that plays a role in PA cell-to-cell communication (quorum sensing) (Dubern and Diggle 2008). It is directly involved in the

synthesis of a family of secondary metabolites, including 4-hydroxy-2-heptylquinoline (HHQ), 2-n-heptyl-4-hydroxyquinoline N-oxide (HQNO) and the *Pseudomonas* quinolone signal (PQS). HHQ, HQNO and PQS have previously been suggested to be inhibitory against a variety of bacterial and fungal species (Hoffman et al. 2006; Orazi and O'Toole 2017; Ramos et al. 2020; Toyofuku et al. 2010). Here, we tested whether they also inhibit our SA strains by focusing on PQS as one of the molecules synthetized by PqsA. We exposed all three SA strains to increasing concentrations of synthetic PQS and found a dose-dependent reduction in growth (Figure 2). This indicates that PQS is involved in the SA growth inhibition that we observed in our supernatant assays.

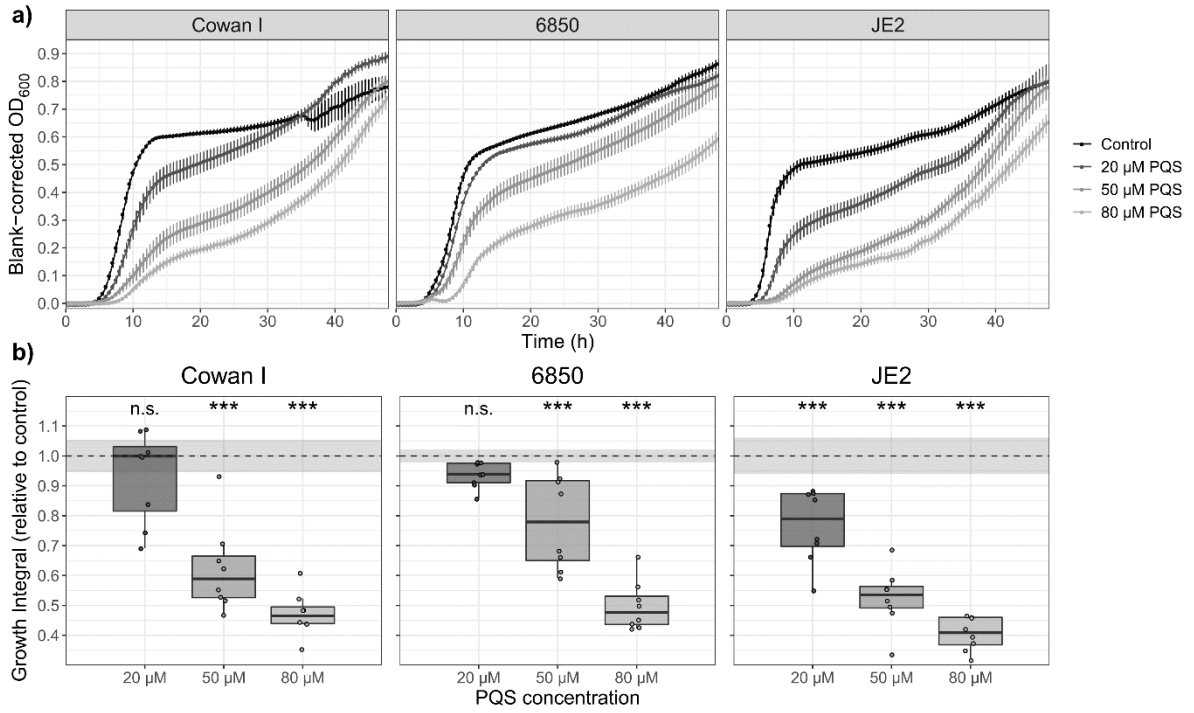

Figure 2. Synthetic PQS suppresses the growth of all three SA strains. SA strains Cowan I, 6850 and JE2 were grown in the presence of increasing concentrations of PQS (20 µM, 50 µM, 80 µM) and OD_{600} was recorded over 48 hours at 37 °C. As a control, we used TSB containing the same volume of DMSO as the 80 µM PQS condition (labelled as 'control', black). (a) Growth trajectories of the three different SA strains in the presence of increasing concentrations of PQS, shown as means ± standard errors. (b) Integrals over the growth trajectories of the three SA strains, relative to the control (dotted line at 1.0 ± 95% confidence interval depicted as shaded area). Box plots show the median (bold line), the first and third quartiles, and the 1.5* inter-quartile range (IQR, whiskers) or the range from the lowest to highest value if all values fall within the 1.5* IQR. Asterisks denote significant differences from the control as determined by Tukey's HSD. *** $p < 0.001$; n.s. not significant. Data are from two independent experiments with eight replicates in total per SA strain and condition.

All SA strains evolve resistance to PA supernatant inhibition

We then asked whether SA can adapt to the PA-induced growth inhibition. This is conceivable because the PA supernatant shows anti-bacterial activity, and one could expect SA to evolve resistance against this activity, in similar ways as pathogens evolve resistance against clinically administered antibiotics. To address this question, we performed an experimental evolution experiment, during which we exposed the three SA strains to either 30% PA supernatant in 70% TSB or to 100% TSB over 30 days, in seven-fold replication (Figure S4). Every 48 hours, we transferred evolving cultures into fresh medium (30% PA supernatant in TSB or 100% TSB) using a 1:10,000 dilution. After experimental evolution, we quantified the growth of evolved populations and randomly isolated evolved clones (five clones per replicate = 210 clones in total) in both experimental media.

We found that populations that had evolved in the presence of PA supernatant showed significantly improved growth performance compared to their respective ancestors when exposed to the PA supernatant, indicating the evolution of resistance (Figure 3a, Cowan I: t_{12} = 11.41, $p < 0.0001$; 6850: t_{12} = 6.31, $p = 0.0002$; JE2: t_{12} = 3.61, $p = 0.0072$). Conversely, all populations that evolved in 100% TSB were still fully or even more susceptible to the PA supernatant compared to the ancestor (Figure 3a, Cowan I: t_{12} = -3.98, $p = 0.0055$; 6850: t_{12} = 1.00, $p = 0.4039$; JE2: t_{12} = -0.87, $p = 0.4368$). Next, we tested whether evolved populations showed TSB-specific adaptations. In support of this view, we found that populations of Cowan I and JE2 that evolved in 100% TSB significantly increased their growth in this medium, but not 6850 (Figure 3b, Cowan I: t_{12} = 11.09, $p < 0.0001$; 6850: t_{12} = -0.77, $p = 0.4590$; JE2: t_{12} = 3.70, $p = 0.0072$). In contrast, populations of all three SA strains that evolved in the presence of PA supernatant did not show improved growth in TSB (Figure 3b, Cowan I: t_{12} = 2.32, $p = 0.0663$; 6850: t_{12} = 1.41, $p = 0.2467$; JE2: t_{12} = 1.94, $p = 0.1137$). These results show that all three SA strains have specifically adapted to the presence of PA supernatant and not merely to TSB, and that these adaptations nullify the growth inhibition originally imposed by the PA supernatant.

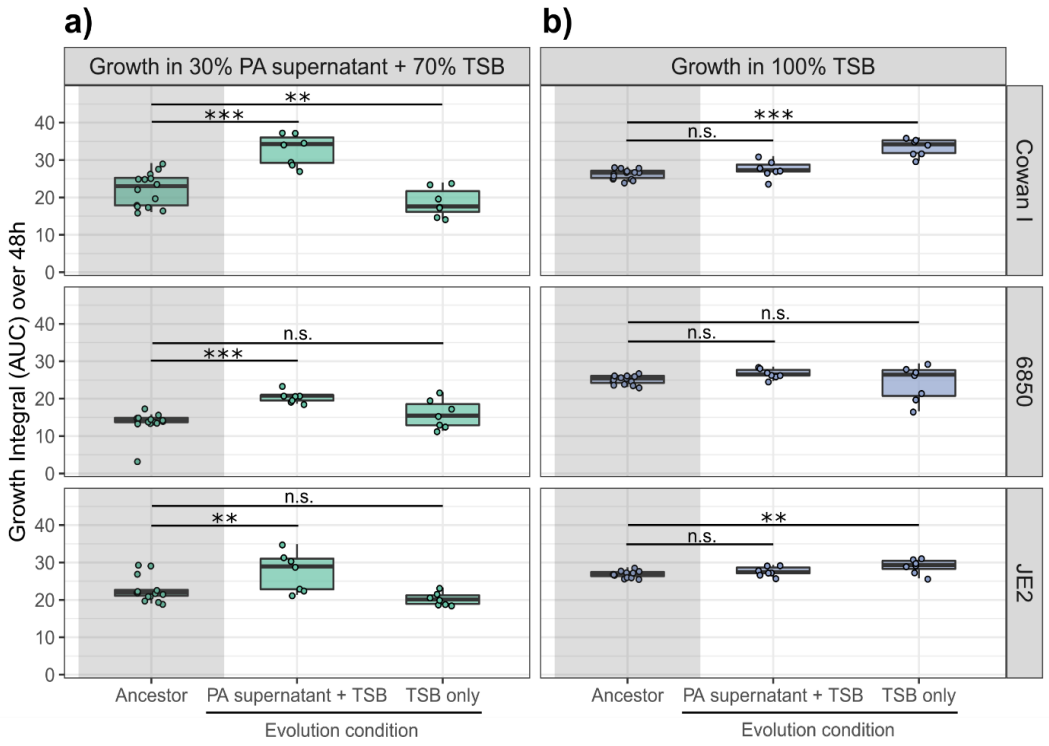

Figure 3. All three SA strains (Cowan I, 6850 and JE2) evolved resistance to inhibitory molecules produced by PA when exposed to its supernatant during experimental evolution (measured as growth integrals over 48 hours, area under the curve). Populations of SA strains either evolved in 30% PA supernatant + 70% TSB or 100% TSB over 30 days with transfer to fresh medium every 48 hours. a) Growth of ancestral (grey-shaded area) and evolved populations in medium containing 30% PA supernatant + 70% TSB. SA populations evolved in the presence of PA supernatant significantly improved growth, while populations evolved in TSB alone are still inhibited by the supernatant. b) Growth of ancestral (grey-shaded area) and evolved populations in 100% TSB medium. SA populations evolved in the presence of PA supernatant did not improve growth in TSB alone, while populations evolved in TSB did so for two of the three SA strains. Box plots show the median (bold line), the first and third quartiles, and the 1.5* inter-quartile range (IQR, whiskers) or the range from the lowest to highest value if all values fall within the 1.5* IQR. Asterisks denote significant differences between the ancestral and evolved populations. *** $p < 0.001$; ** $p < 0.01$; n.s. not significant. P-values are adjusted by the false discovery rate method.

We then repeated all the above growth assays with the 210 individual clones. The results confirmed our population-level analysis (Figure S5). Overall, we observed considerable variation among clones in their growth phenotype. This suggests that populations are heterogenous, consisting of multiple different genotypes, an aspect we confirm in our phenotypic and genomic analyses below.

Clones evolved in the presence of PA supernatant overproduce staphyloxanthin (STX)

From an infection perspective, it is important to understand whether adaptation to a competitor involves traits that also affect the host and could have consequences for virulence. We therefore screened our collection of evolved clones for changes in phenotypes, which we anticipated to be involved in resistance evolution towards PA supernatant and are known to have virulence consequences. We restricted our analysis to 150 clones from 30 out of the 42 populations, as this sample size matched our genomic sequencing contingent.

At first, we quantified the production of staphyloxanthin (STX), the golden carotenoid pigment. STX acts as an antioxidant and virulence factor (Clauditz et al. 2006), and could be under selection in the presence of PA (Antonic et al. 2013). We found that STX production changed during the course of evolution (Figure 4a) and was significantly higher in clones that evolved in the presence of PA supernatant than in clones evolved in TSB alone (ANOVA: $F_{1,146} = 16.37$, $p < 0.0001$). Moreover, there were significant differences between SA strains ($F_{2,146} = 22.93$, $p < 0.0001$). While all clones of 6850 and JE2 that evolved in PA supernatant had increased STX production compared to the ancestor, the same was true only for a fraction of Cowan I clones. In TSB alone, evolved clones from Cowan I even showed decreased STX production relative to the ancestor, whereas many of the evolved 6850 clones (and some JE2 clones) also increased STX production under this evolution condition. These analyses show that STX production is generally under selection in TSB but reaches particularly high levels in the presence of PA supernatant.

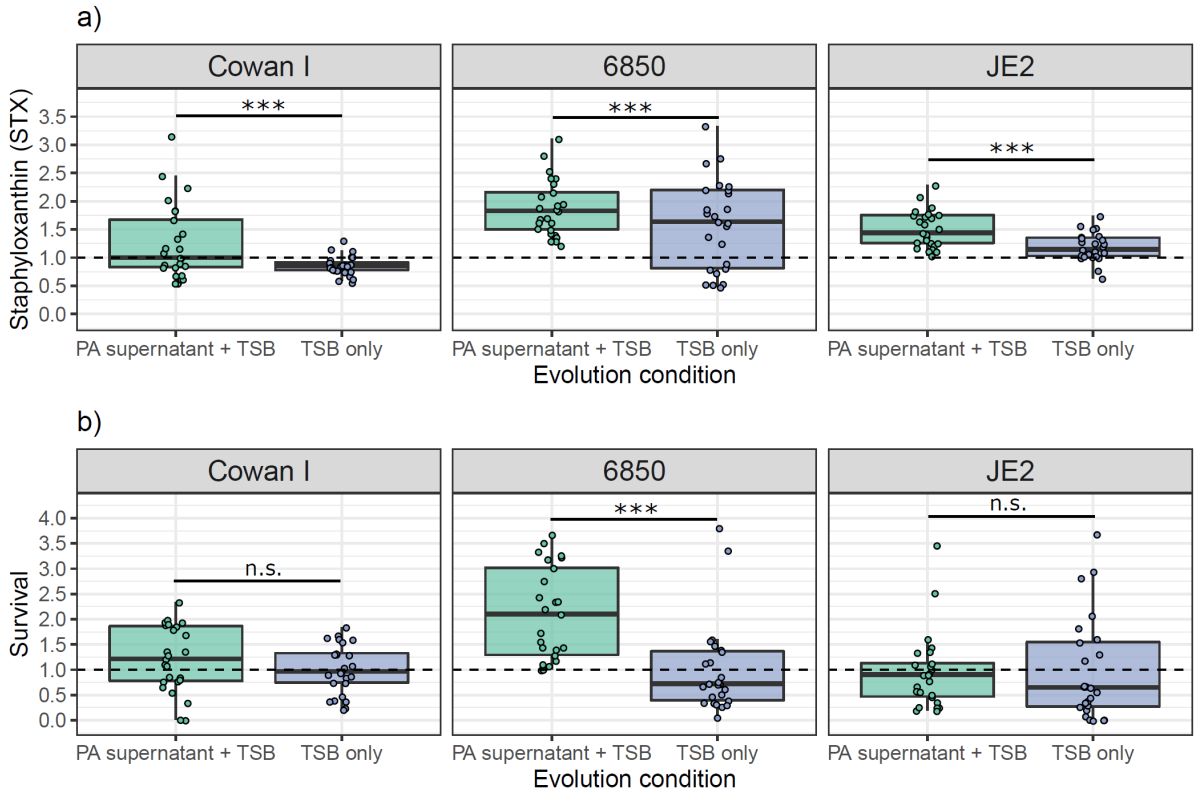

Figure 4. Change in staphyloxanthin (STX) production and survival in the presence of hydrogen peroxide (H_2O_2) during experimental evolution varies across SA strains and between media conditions. a) Production of STX for evolved clones from Cowan I, 6850 and JE2, expressed relative to the respective ancestor (dashed line at 1.0). STX was assessed by measuring the absorbance of the crude extract containing STX for 150 evolved clones (25 clones from 5 populations per strain and condition) at λ = 465 nm. b) Survival of evolved clones from Cowan I, 6850 and JE2 after exposure for one hour to 1.5% H_2O_2, expressed relative to the respective ancestor (dashed line at 1.0). Survival was measured as the number of colony forming units on TSB + 1.2% agar plates relative to an unchallenged control for the same 150 clones. Every dot represents the average value from two independent STX extractions and survival assays per clone. Box plots show the median (bold line), the first and third quartiles, and the 1.5* inter-quartile range (IQR, whiskers) or the range from the lowest to highest value if all values fall within the 1.5* IQR. Asterisks denote significant differences between the two evolution conditions for each SA strain (Tukey's HSD with adjusted p-values). *** $p < 0.001$; n.s. not significant.

Adaptation towards oxidative stress is SA strain specific

Inhibitory molecules from the PQS system can cause oxidative stress in target cells (Abdalla et al. 2017; Bredenbruch et al. 2006; Tognon et al. 2019) and we therefore wondered whether clones that evolved in the presence of PA supernatant are more resistant towards oxidative stress. Thus, we exposed all clones and the respective ancestors for one hour to a 1.5%

hydrogen peroxide (H_2O_2) solution and determined their survival compared to the unstressed control. We observed that the survival of evolved SA clones depended on a significant interaction between strain background and experimental medium (ANOVA: $F_{2,144} = 6.81$, $p = 0.0015$, Figure 4b). This interaction is driven by 6850, as for this strain clones evolved in the presence of PA supernatant survived significantly better than clones evolved in TSB alone. No such significant treatment effects were observed for Cowan I and JE2 clones.

Since the carotenoid pigment STX is involved in protection against reactive oxygen species (Xue et al. 2019), we tested whether clones with increased STX production showed higher survival in the presence of H_2O_2. Indeed, we found a positive correlation between STX production and survival for clones evolved in the presence of PA supernatant (Pearson's product-moment correlation, $r_{73} = 0.27$, $p = 0.0207$, Figure S6a), but not for clones evolved in TSB alone ($r_{73} = -0.02$, $p = 0.8920$, Figure S6b). In sum, the survival data highlights that the three SA strains differ in their adaptation towards PA supernatant and that evolved clones of 6850 showed the highest improvements in both STX production and survival rate.

Formation of small colony variants in the presence of PA supernatant

As small colony variants (SCVs) offer protection from stressful conditions, including reactive oxygen species (Biswas et al. 2009; Hoffman et al. 2006; Kahl, Becker, and Löffler 2016; Tuchscherr et al. 2011), we anticipated increased SCV formation to be another evolutionary response of SA towards inhibitory molecules produced by PA. Consequently, we tested whether SCV frequency increased during experimental evolution. Screening for SCVs is difficult, as colony size is a variable trait and phenotypic unstable SCVs can quickly revert back to regular colony sizes (Leimer et al. 2016). Our first screen involved the plating of evolved populations on agar plates to detect the presence of SCVs. We found SCVs in five out of seven Cowan I populations that had evolved in the presence of PA supernatant (Figure S7). SCVs also surfaced in populations of other strains and media, but at a reduced rate (Cowan I in TSB [2 out of 7 populations]; 6850 in TSB [1/7]; JE2 in PA supernatant + TSB [1/7]).

The above screen suggests that SCV formation occurs most commonly in Cowan I in response to PA supernatant exposure. For this reason, we screened all evolved clones from this evolution condition and found that five out of the 25 Cowan I clones expressed a SCV phenotype. We classified three and two of these clones as dynamic/unstable and stable SCVs, respectively. Dynamic/unstable SCVs consistently formed two colony types (small and normal-sized colonies) upon repeated re-streaking. When comparing their growth trajectories in PA supernatant + TSB to the Cowan I ancestor, they had a shorter lag phase and a higher yield (Figure 5a). The two stable SCVs had a longer lag phase and a lower yield than the normal-sized clones isolated from the same population. However, the death phase observed in the Cowan I ancestor was abrogated, suggesting that stable SCV formation increases survival under stressful conditions (Figure 5b). From these analyses, we conclude that both dynamic/unstable and stable SCV formation can be adaptive strategies. While the former increases overall growth performance, the latter prevents cell death at high population density.

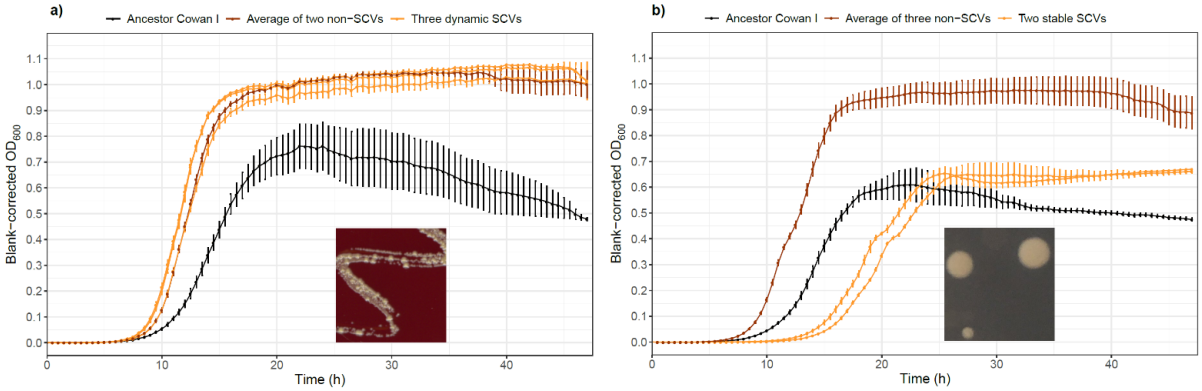

Figure 5. Characteristics of the five small colony variants (SCVs) evolved in the Cowan I background. a) Growth trajectories of the three dynamic/unstable SCVs in 30% PA supernatant + 70% TSB. Compared to the Cowan I ancestor, dynamic/unstable SCVs have a shorter lag phase and a higher yield, which is similar to the normal-sized clones isolated from the same population. The inset shows one of the dynamic/unstable SCVs with the two colony types on a sheep blood agar plate. b) Growth trajectories of stable SCVs in 30% PA supernatant + 70% TSB. Compared to normal-sized clones from the same population, the two stable SCVs have a longer lag phase and a lower growth yield, but they no longer show the decrease in OD_{600} that is characteristic for the Cowan I ancestor. The inset shows a stable SCV (bottom-left) compared to two normal-sized colonies (upper left and right) from the population from which the two stable SCVs were isolated. Curves show the average growth (± standard error) across 4 replicates.

The presence of PA supernatant maintains hemolysis

Hemolysis (lysis of red blood cells) is an important virulence-related phenotype in SA, and its expression is regulated in complex ways, including the accessory gene regulator (agr) system and other regulatory genes (Burnside et al. 2010). The loss of hemolysis has repeatedly been observed in SA isolates from chronic infections (Shopsin et al. 2008; Traber et al. 2008).

Here, we asked whether the presence of PA supernatant affects the evolution of this phenotype in 6850 and JE2 (Cowan I is a non-hemolytic SA strain, due to partial agr dysfunctionality). Our population (Figure S8) and clonal (Figure 6) level analysis show that the majority of 6850 and JE2 clones and populations remained hemolytic after evolution in PA supernatant + TSB. In contrast, after evolution in 100% TSB, hemolytic activity only remained high in clones from 6850 (72% still showed ancestral activity, Figure 6a), while 84% of the JE2 clones lost their hemolytic activity (Figure 6b), a pattern that was also reflected at the population level (Figure S8). These findings show that the presence of PA supernatant fosters the maintenance of hemolysis, and that the speed by which hemolysis can be lost depends on the SA strain genetic background.

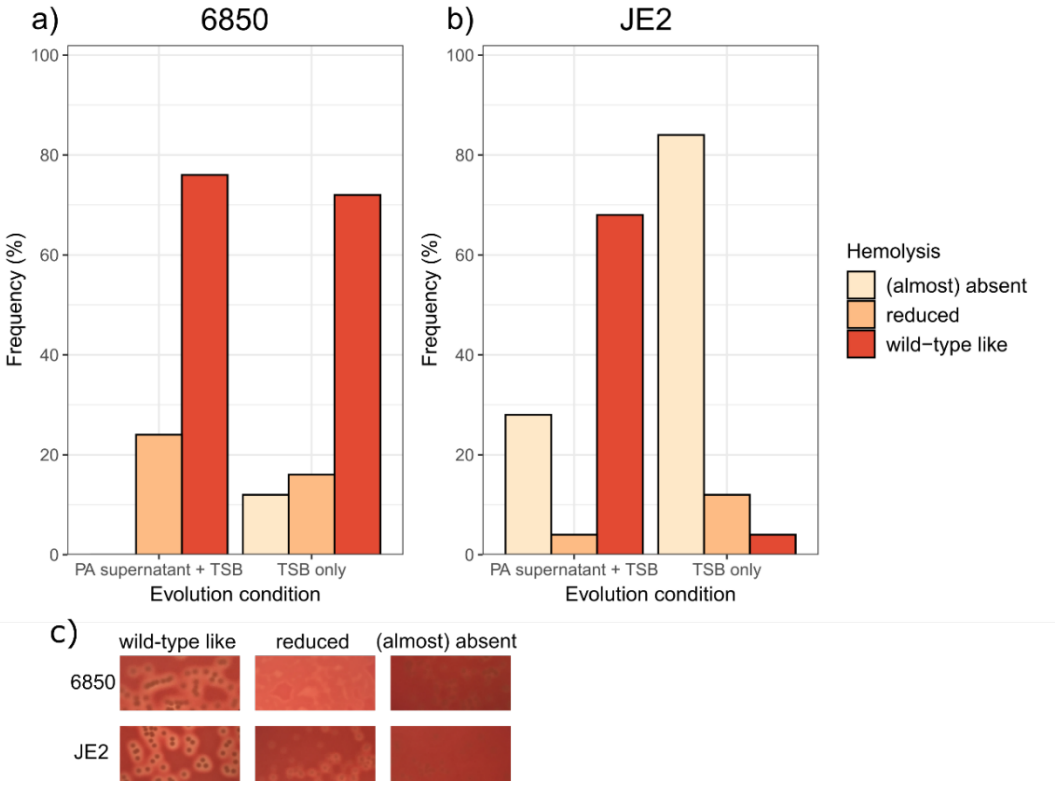

Figure 6. The PA supernatant selects for the maintenance of hemolysis in JE2. 100 evolved clones were plated on sheep blood agar plates to score their hemolysis levels according to three categories: wild-type like (ancestral), reduced, (almost) absent. Note that the Cowan I ancestor is non-hemolytic and therefore not part of this assay. a) Frequency of the three hemolysis categories for the evolved 6850 clones. There is no significant difference in the hemolysis profiles between clones evolved in PA supernatant + TSB versus in TSB only (Fisher's exact test: $p = 0.2266$) and most clones remained hemolytic. b) Frequency of the three hemolysis categories for the evolved JE2 clones. There is a significant difference in the hemolysis profiles between clones evolved in PA supernatant + TSB versus in TSB only (Fisher's exact test: $p < 0.0001$). The large majority of JE2 clones evolved in TSB only are no longer hemolytic. c) Representative pictures of the three hemolysis categories for the SA strains 6850 and JE2.

SA strains follow divergent and medium-specific evolutionary trajectories

We performed a principal component analysis (PCA) to statistically test whether the observed phenotypic changes are SA strain background and/or media specific. The following four phenotypes of 150 evolved clones were integrated into the PCA: (i) growth in 100% TSB; (ii) growth in 30% PA supernatant + 70% TSB; (iii) STX production; and (iv) survival in the presence of oxidative stress. We found that evolved clones significantly clustered based on the evolution condition (PERMANOVA; $F_{1,144} = 36.59$, $p = 0.0010$, Figure 7), strain background ($F_{2,144} = 24.06$, $p = 0.0010$), and their interaction ($F_{2,144} = 11.79$, $p = 0.0010$). The PCA therefore clearly supports our notion that evolutionary trajectories differ across SA strain background and media.

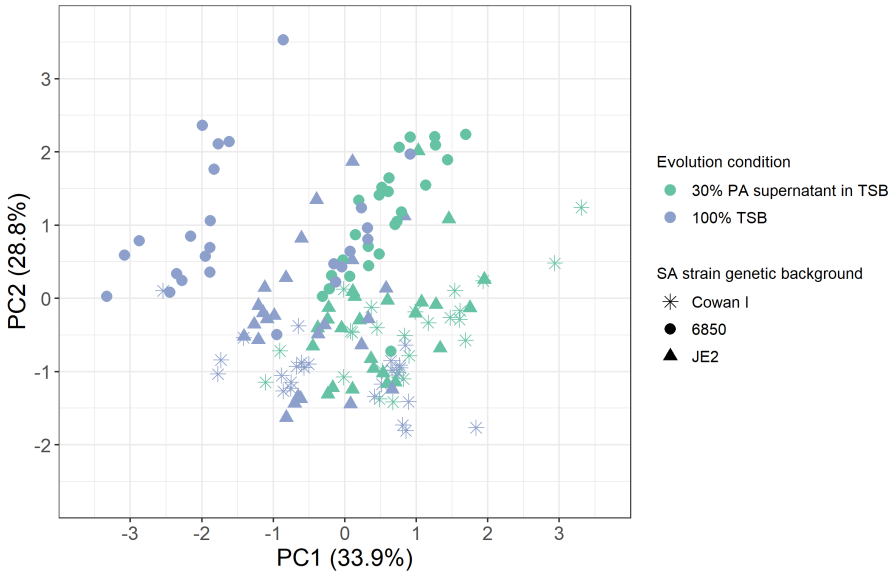

328 **Figure 7.** Principal component analysis (PCA) on the phenotypes of 150 evolved clones reveals strain
329 and media specific evolutionary divergence. The following four phenotypes were integrated into the
330 PCA: growth in 30% PA supernatant + 70% TSB, growth in 100% TSB, staphyloxanthin production and
331 survival in the presence of oxidative stress. The first two principal components (PC1 and PC2) explain
332 62.7% of the total variance in the data set. Statistical analyses reveal significant divergences in the
333 evolved phenotypes between the three SA strains (Cowan, 6850, JE2), and the condition they evolved
334 in (30% PA supernatant + 70% TSB, 100% TSB).
335

336 **Mutational patterns of evolved clones are media-specific**

337 To identify the genetic basis of the observed evolutionary changes, we sequenced the genome
338 of all the 150 evolved clones for which we collected the above phenotypes, and the three SA
339 ancestors Cowan I, 6850 and JE2. Compared to the ancestors, we identified nonsynonymous
340 mutations in 119 different genes and mutations in 51 different intergenic regions across all
341 evolved clones. Among those, 68 and 109 genes or intergenic regions were mutated in clones
342 that had evolved in PA supernatant + TSB and in 100% TSB, respectively. The large majority
343 (96.6%) of the 119 genes with nonsynonymous mutations occurred uniquely in one of the two
344 media (either in PA supernatant + TSB or 100% TSB), and there was little overlap in mutational
345 targets between strains (Figure 8a). These results are in line with our phenotypic assays,
346 highlighting that each SA strain followed a divergent evolutionary trajectory in each of the two
347 media.

348 For all three SA strains, the median number of mutations was lower for clones evolved
349 in PA supernatant + TSB than in 100% TSB (Cowan I: 2.0 vs. 4.0; 6850: 1.0 vs. 4.0; JE2: 2.0
350 vs. 5.0, Figure 8b), indicating that fewer mutations were beneficial in the presence of PA
351 supernatant than in TSB alone. The ratio of nonsynonymous to synonymous SNPs (dN/dS)
352 was higher than one for all strains and in both media (dN/dS for Cowan I: PA supernatant +
353 TSB / 100% TSB = 3.1 / 2.5; for 6850: 13.0 / 12.0; for JE2 3.6 / 4.0). These results show that
354 positive selection and adaptive evolution occurred in both conditions.

355 To determine whether the mutational patterns differed between the two media and the
356 three SA strains in terms of the functional classes affected, we sorted the mutated genes using
357 aureowiki (Fuchs et al. 2018) and the primary literature. Indeed, in clones that evolved in the

358 presence of PA supernatant, we found an enrichment of mutated genes belonging to the
359 category ‘membrane transporter’, while for clones that had evolved in TSB alone, most
360 mutated genes belonged to the categories ‘metabolism’, ‘cell wall organization’ and ‘signal
361 transduction’ (Figure 8c).
362

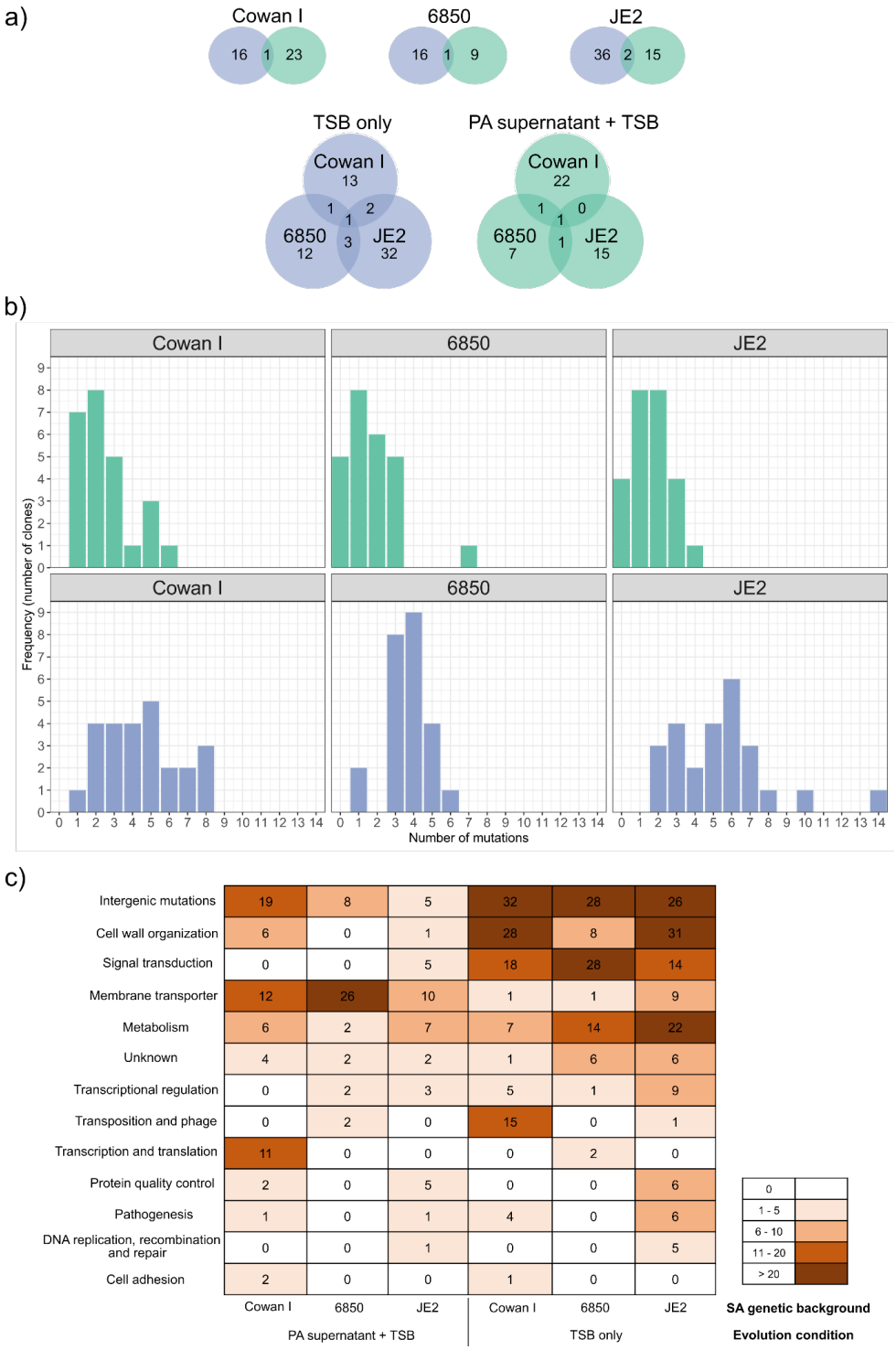

363

Figure 8. Genomic analysis of 150 evolved clones reveals strain and media specific mutational patterns. a) Venn diagrams showing how often genes with nonsynonymous mutations are unique to or shared between evolution conditions (top row) and the three SA ancestors (bottom row). There is little overlap among mutated genes, indicating that most mutations are unique to the specific evolution condition and SA strain. b) Number of mutations per clone (nonsynonymous and intergenic mutations) split according to SA strain background (Cowan I, 6850, JE2) and evolution condition (green: 30% PA supernatant + 70% TSB; blue: 100% TSB). Clones evolved in the presence of PA supernatant had significantly fewer mutations than clones evolved in TSB alone. c) Heatmap showing the total abundance of mutations in functional gene categories and intergenic regions (top row) across all sequenced clones, split by SA strain background (Cowan I, 6850, JE2) and evolution condition (30% PA supernatant + 70% TSB or 100% TSB). Note that we counted every mutation in every clone for this latter analysis.

Parallel evolution in TSB, diverse non-parallel evolution in PA supernatant

Next, we explored whether there is evidence for parallel evolution, which should manifest in similar mutational patterns surfacing across independently evolved populations and strains. For this purpose, we identified genes that mutated more than once in at least two populations/strains. Across both evolution conditions, we found 11 genes that fulfilled these criteria (Table S2). When focusing on the TSB alone medium, there were three genes (*fmtA*, *gdpP*, *walK*) that stood out in terms of both their frequency of mutations and distribution across SA strains. The teichoic acid D-Ala esterase *fmtA* mutated in five Cowan I populations, one 6850 population, and five JE2 populations [5/1/5]. Mutations in the cyclic-di-AMP phosphodiesterase *gdpP* [0/4/5] and the cell wall histidine kinase *walK* [5/3/0] were similarly frequent. A striking pattern is that mutations in any of these three genes are only common in two out of the three SA strains in changing combinations. These results demonstrate that (i) there is high level of parallel evolution between populations of the same strain; (ii) there is a certain level of parallel evolution across strains but the combination of genes that are under selection varies; and (iii) mutations in *fmtA*, *gdpP* and *walK* are likely involved in general adaptations to the TSB medium, as these genes are not under selection in the PA supernatant treatment.

For populations evolved in PA supernatant + TSB, we found a different pattern. Only the gene *alsT* mutated in all SA strain backgrounds (Cowan I [2 populations], 6850 [3], JE2

[1]), with *alsT* mutations occurring in a total of 22 clones. This suggests that mutations in *alsT*, which encodes a glutamine transporter (Zeden et al. 2020), are generally advantageous in the presence of PA supernatant. The lack of any other evidence for parallel evolution indicates that SA populations of all strains adapted to PA supernatant in a highly diverse and individual manner.

Absence of strong associations between evolved genotypes and phenotypes confirms highly diverse evolutionary trajectories in response to PA inhibitory molecules

We used the mutational patters uncovered to construct evolutionary cladograms for each population independently evolved in the presence of PA supernatant. Additionally, we mapped three phenotypes (growth in PA supernatant + TSB, staphyloxanthin [STX] production, hydrogen peroxide [H_2O_2] survival) onto the cladograms to identify links between genotypic and phenotypic changes (Figure 9).

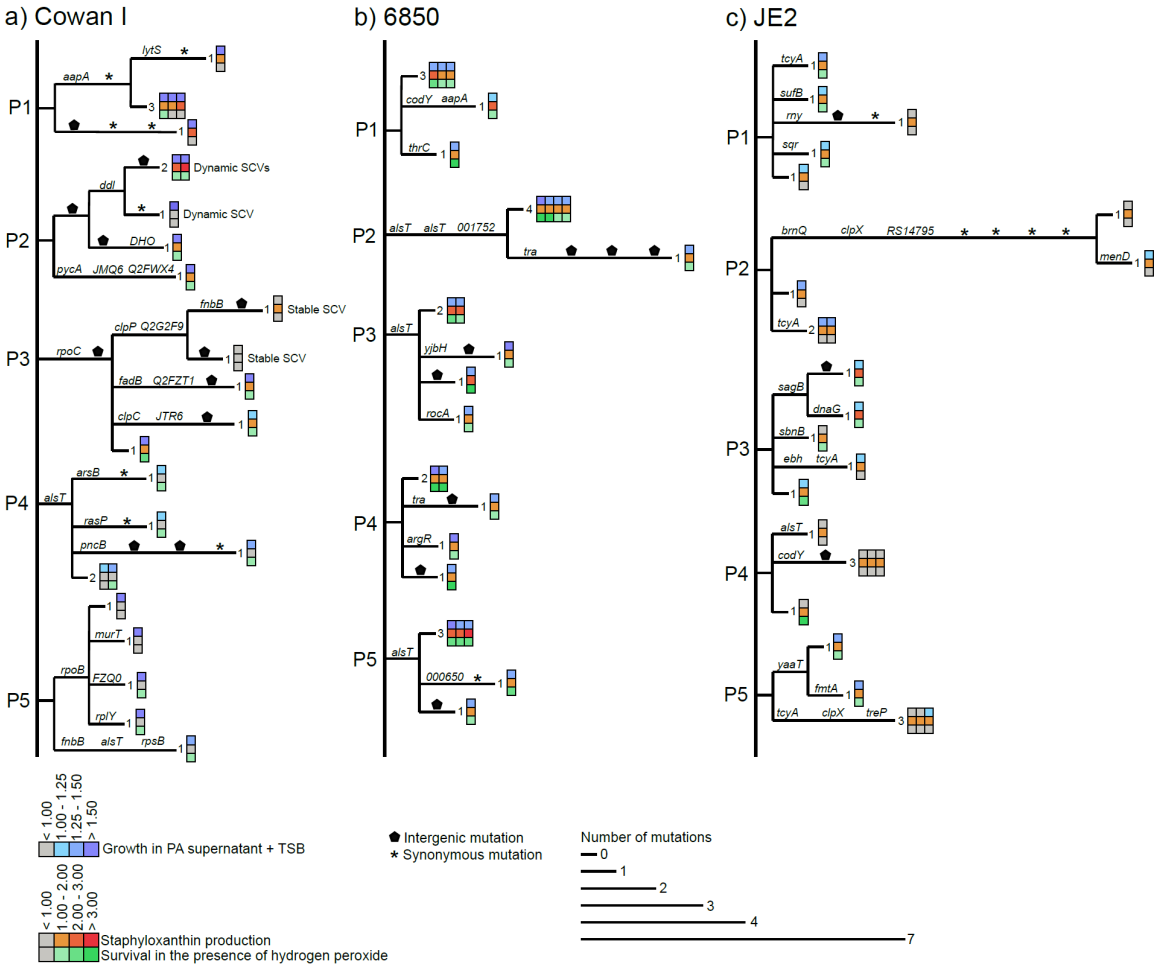

Figure 9. Cladograms showing within-population mutational patterns and their match to phenotypes of SA clones evolved in the presence of PA supernatant. Separate cladograms are shown for each of the five populations (P1 – P5) of the three SA strains (a) Cowan I, (b) 6850, and (c) JE2. Branch length corresponds to the number of mutations per clone. Labels on branches indicate either nonsynonymous mutations (gene name or abbreviated locus tag), intergenic mutations (pentagon), or synonymous mutations (asterisk). Synonymous mutations were used to resolve branching patterns among clones. Heatmaps on the tip of the branches show growth in the presence of PA supernatant (top row), staphyloxanthin production (middle row), and survival in the presence of hydrogen peroxide (bottom row) for the respective evolved clones, all expressed relative to the ancestor.

For Cowan I (Figure 9a), mutational patterns were highly diverse within and across populations and there was no apparent link to any of the phenotypes. For example, while 23 out of 25 clones showed resistance to PA supernatant in terms of growth, the underlying mutational patterns were extremely diverse.

For 6850 (Figure 9b), there is some evidence for parallel evolution via mutations in *alsT*, which became fixed in three different populations. All clones with *alsT* mutations showed higher growth, increased STX production and H_2O_2 survival. However, the same phenotypic changes were also observed in other 6850 clones without *alsT* mutations. This shows that mutations in different genes can lead to the same phenotypic changes.

For JE2 (Figure 9c), the genotype-phenotype matching was diverse, too. Overall, JE2 showed the least pronounced changes in phenotypes, most likely because the ancestor was least affected by the PA supernatant (Figure 1). But when focusing on the clones in populations P1, P3 and P5, which showed the most pronounced increases in growth, STX production and H_2O_2, we found completely different underlying mutational patterns in each population. For example, mutations in *tcyA* (population P1), *sagB* (P3), and *yaaT* (P5) all seemed to be associated with the altered phenotypes. Only the *tcyA* gene, encoding a membrane transporter, stood out from the other genes as it was repeatedly mutated in seven clones from four different JE2 populations, suggesting that it plays a more general role in SA resistance evolution.

Discussion

Pseudomonas aeruginosa (PA) and *Staphylococcus aureus* (SA) are among the most important pathogens in polymicrobial infections, such as cystic fibrosis (CF) lung and wound infections, and there is high interest in understanding how their interactions shape disease outcome (Ibberson and Whiteley 2020; Limoli and Hoffman 2019). A large body of literature has examined PA-SA interactions at the molecular level, and mostly described PA as the dominant species suppressing the growth of SA by producing a variety of inhibitory molecules (Hotterbeekx et al. 2017). However, because polymicrobial infections containing PA and SA are often chronic, the two species may interact with each other (and with the host) over prolonged periods of time, which could spur co-evolutionary dynamics, and the possibility of SA to adapt to PA inhibitory molecules (Camus et al. 2021; Serra et al. 2015). Here, we tested this hypothesis by exposing three different SA strains (Cowan I, 6850 and JE2) to the supernatant, containing inhibitory molecules, of the PA reference strain PAO1, during experimental evolution over 30 days. We found that all SA strains rapidly evolved resistance to the growth inhibition imposed by PA. Using a combination of phenotypic and genotypic assays, we show that (i) resistance evolution affected virulence traits, including increased staphyloxanthin (STX) expression, higher survival in the presence of oxidative stress, small colony variants (SCV) formation, and the maintenance of hemolysis; (ii) evolutionary trajectories were highly SA strain-specific; and (iii) mutations in genes encoding membrane transporters were the most frequent target of evolution. Our findings not only show that SA can rapidly adapt to inhibitory molecules of PA, but also reveal that SA upregulates virulence traits and modifies membrane transporters in response to PA supernatant exposure, evolutionary changes that could lead to higher virulence and increased antibiotic resistance in infections.

All three SA strains were initially compromised in their growth by the PA supernatant, and we confirmed that the *Pseudomonas* quinolone signal (PQS) molecule was directly involved in growth inhibition. PQS does not only serve as a quorum-sensing signaling molecule but also functions as an iron trap (Diggle et al. 2007). The iron-chelating activity of PQS reduces the bioavailability of iron in the environment, and is known to inhibit a variety of gram-

negative and gram-positive bacterial species (Popat et al. 2017; Toyofuku et al. 2010). Here, we show that it also has a strong inhibitory effect on SA. HQNO is another molecule produced through the PQS synthesis cascade that has anti-SA properties via inhibition of the respiratory chain (Hoffman et al. 2006). It is thus likely that the inhibitory effects on SA growth observed in our supernatant assays is a combination of the effects of PQS and HQNO.

We found that the extent to which SA strains were inhibited and the strength of resistance evolution towards the PA supernatant varied across SA strains (Figure 3). While the Cowan I ancestor was greatly inhibited, it showed the largest improvement in growth after evolution in the PA supernatant, and even outperformed the ancestral wildtype growing in TSB alone. Similarly, 6850 was initially greatly inhibited by the PA supernatant, and all replicate populations showed resistance evolution, reflected by a significantly improved growth. JE2 was initially the least inhibited strain, and while overall, we found significantly improved growth after evolution, not all replicate populations followed this trend. It is perhaps unsurprising that the most severely affected SA strains showed the strongest response in terms of resistance evolution. However, it is interesting that the ancestral JE2 is the most virulent and most competitive SA strain in our panel (Diep et al. 2006; Niggli and Kümmerli 2020). This suggests that JE2 might already be well equipped to deal with PA inhibitory molecules, leaving less room for further fitness improvements compared to the less virulent and less competitive Cowan I or 6850 strains.

During evolution, we observed that SA virulence traits were under selection and often overproduced, which could have severe consequences in infections (Cheung, Bae, and Otto 2021; Pollitt et al. 2014). Importantly, the virulence traits under selection varied across SA strains, reinforcing our notion that evolutionary responses to PA inhibitory molecules are SA strain specific. Increased formation of SCVs evolved almost exclusively in Cowan I populations. However, we assume that the true SCV frequency might be higher than the one reported, because SCVs are difficult to detect. The formation of SA SCVs is a well-known adaptive response towards stressful conditions (Kahl, Becker, and Löffler 2016), and we propose that SCVs evolved in our experiment as a response to PA inhibitory molecules such

as HQNO (Hoffman et al. 2006). Due to their slow metabolism, SCVs frequently exhibit reduced antibiotic susceptibility, which makes them particularly problematic in a clinical context (Huemer et al. 2020). For 6850 clones, the strongest phenotypic changes involved increased STX production and better survival in the presence of oxidative stress (H_2O_2 exposure). Adaptations in 6850 therefore likely led to better protection against reactive oxygen species (ROS) induced by PA inhibitory molecules, such as HQNO, pyocyanin, and PQS (Abdalla et al. 2017; Noto et al. 2017; Tognon et al. 2019). In the context of infections, such adaptations would be problematic, because innate host immune responses against pathogens typically involve the production of ROS (Schieber and Chandel 2014). For JE2, we observed that hemolysis was selectively maintained in the presence of PA supernatant but lost in its absence. While hemolysis is an important virulence trait, it can be lost in chronic infections (Shopsin et al. 2008; Traber et al. 2008). Our findings now suggest that the presence of PA could maintain this trait and keep JE2 and related strains at a higher state of virulence.

At the genetic level, we found positive selection but little evidence for parallel evolution across strains and populations upon exposure to the PA supernatant. This indicates that mutations in many different genes were under selection and possibly contributed to resistance evolution towards PA inhibitory molecules. The fact that mutations in a broad spectrum of genes can promote resistance highlights the enormous evolvability of SA (Deurenberg and Stobberingh 2008). In contrast, we found evidence for parallel evolution among clones that evolved in the TSB medium alone, where we identified several genes (Table S2) that were frequently mutated in independent populations and across strains. These findings show that, whether or not parallel evolution occurs, depends on the environment and the specific selection pressures that prevail therein.

Remarkable is that, although there was little evidence for parallel evolution at the gene level in clones evolved in the presence of PA supernatant, we found parallelism at the functional level, with many mutations occurring in membrane transport genes (Figure 8c). For example, the gene encoding the glutamine transporter AlsT was mutated in 22 clones from six populations across all three SA strains. While AlsT inactivation reduces the susceptibility of

SA to the toxic glutamine analogue γ-L-glutamyl hydrazide (Zeden et al. 2020), our results now suggest that AlsT alterations might similarly reduce the uptake of PA inhibitory molecules. Moreover, it was shown that loss-of-function mutations in *alsT* increase intracellular c-di-AMP levels, which allows bacteria to better resist stressful conditions (Corrigan et al. 2011). Our results support this notion and suggest that *alsT* mutations were selected for to withstand the stress imposed by PA inhibitory molecules in the supernatant. Another example involves mutations in the gene *tcyA*, which encodes a part of the cystine transporter TcyABC. While mutations in this gene were unique to JE2, they surfaced in seven clones in four out of the five JE2 populations. Deletion of *tcyA* leads to resistance against the toxic cystine analogue selenocystine in SA (Lensmire et al. 2020). While PA strain PAO1 indeed contains the selenocysteine synthesis cluster, it is currently not known how its expression is controlled and whether selenocystine is deployed against competitors. Our data now suggest that it might indeed play a role in competition, and that mutations in *tcyA* could be an evolutionary response by SA to reduce selenocystine uptake. More generally, as membrane transport systems are known to control virulence and antibiotic resistance in SA, they have been proposed as novel targets for therapeutic agents (Zeden et al. 2021). Our finding that the exposure to PA inhibitory molecules can select for SA variants with altered membrane transporters could therefore pose a problem for drug design and therapy, as these mutants could be less susceptible to antibiotics.

In summary, our work shows that SA rapidly and specifically adapts to PA inhibitory molecules. Several virulence traits were upregulated or selectively maintained in response to PA supernatant exposure, and our genomic analysis revealed that mutations in membrane transport genes are associated with resistance evolution in SA. Such adaptations could have severe implications for infections, as SA virulence might be increased, and baseline levels of antibiotic resistance might arise even before a treatment is applied. A key next step would involve testing whether the observed increases in virulence trait expression and mutations in membrane transporters lead to altered virulence and antibiotic susceptibility profiles *in vivo*. Moreover, while we focused on SA evolution and others on PA evolution (Tognon et al. 2017),

552 we next need to study co-evolution to understand the patterns and consequences of reciprocal
553 adaptation in both species, as they might occur in polymicrobial infections (Rezzoagli, Granato,
554 and Kümmerli 2020). In a broader context, the fact that evolutionary trajectories were strongly
555 SA strain-specific, suggests that we ultimately need to understand polymicrobial dynamics and
556 its consequences at an 'individualized' patient-by-patient level to identify optimal personalized
557 treatment strategies for each case.
558
559 **Materials and Methods**
560 **Bacterial strains, media, and growth conditions**
561 We used *Pseudomonas aeruginosa* (PA) strain PAO1 (ATCC 15692) and the three genetically
562 different *Staphylococcus aureus* (SA) strains Cowan I, 6850 and JE2 (Table S1) for all our
563 experiments. All growth experiments and the experimental evolution were performed in tryptic
564 soy broth (TSB, Becton Dickinson, Heidelberg, Germany) medium. Overnight cultures (prior to
565 experimental evolution) were grown in 10 ml TSB in 50 ml falcon tubes at 37 °C and 220 rpm
566 with aeration. The phenotypic assays after experimental evolution involved large sample sizes
567 including many evolved clones, populations, and the respective ancestors. For this reason, we
568 grew overnights in 24-well plates filled with 1.5 ml TSB per well at 37 °C and 170 rpm.
569
570 **Supernatant assays**
571 To test whether the supernatant of PA inhibits SA (and vice versa) we performed supernatant
572 growth assays as follows. We first generated cell-free supernatants by growing PA and SA
573 donor strains overnight in TSB. After centrifugation of the cultures to pellet cells, we sterile-
574 filtered the supernatant using 0.2 µm pore size filters (Whatman, Fisher Scientific, Reinach,
575 Switzerland) and stored aliquots of the supernatant at -20 °C. For the supernatant assay, we
576 grew PA and SA receiver strains overnight, washed bacterial cell pellets with 10 ml 0.8% NaCl
577 and adjusted OD_{600} (optical density at 600 nm) to obtain comparable cell numbers per ml for
578 all strains. To achieve this, we adjusted OD_{600} of PA to 1.0, for SA strains JE2 and 6850 to 0.4
579 and for Cowan I to 0.8. Subsequently, we diluted the PA inoculum 1:100,000 and the SA

inoculums 1:10,000 to start our experiments. PA was diluted more because it grows faster compared to SA. The diluted inoculums were prepared in the following three media conditions: (1) 100% TSB (as growth control); (2) 30% NaCl solution + 70% TSB (control to mimic reduced nutrient availability); (3) 30% PA or SA supernatant + 70% TSB (condition of interest).

Supernatant assays were performed in 96-well plates with 200 µl per well. We incubated plates statically at 37 °C in a plate reader (Tecan Infinite M nano, Tecan, Männedorf, Switzerland) and measured growth of strains by recording OD_{600} every 30 min for 48 hours, with 30 sec shaking events prior to recordings. Effect of PA supernatant on growth of SA strains was assessed in seven independent experiments and effect of SA supernatants on PA growth was assessed in one experiment per SA supernatant. In every assay, we used four replicates per strain and growth condition.

SA growth in the presence of PQS

To test whether PQS (heptyl-3-hydroxy-4(1H)-quinolone, Sigma-Aldrich, Buchs, Switzerland) is involved in the growth inhibition of SA, we exposed cultures of all three SA strains to final concentrations of 20 µM, 50 µM or 80 µM PQS (10 mM stock in DMSO), supplemented to the TSB growth medium, and compared their growth relative to the growth in TSB supplemented with DMSO alone (same volume of DMSO as for the 80 µM PQS treatment). SA strain preparation and growth measurements followed the same protocol as for the supernatant assays.

Experimental evolution of SA in the presence or absence of PA supernatant

To elucidate whether and how SA strains respond to the presence of PA supernatant over time, we performed an experimental evolution experiment, in which we exposed the three SA strains Cowan I, 6850 and JE2 for 30 days to either 30% PA supernatant + 70% TSB (experimental treatment) or 100% TSB (control treatment). Experimental evolution started from clonal populations. We had seven independent populations per strain and condition, resulting in a total of 42 evolving populations, distributed on 96-well plates (one plate per SA ancestor).

All populations were incubated statically at 37 °C. Every 48 hours, we diluted and transferred the evolving cultures 1:10,000 into fresh medium and recorded OD_{600} as a proxy for growth prior to each transfer using a plate reader (Tecan Infinite M nano). To the part of the culture that was not transferred, we added equal volumes of a sterile 85% glycerol solution directly into the wells of the 96-well plate and froze them at -80 °C as a backup. Overall, the experiment ran for 30 days (15 transfers). Based on a pre-experiment, we estimated the mean number of doublings (± standard deviation) for the three SA ancestors in the two growth conditions during a 48-hour growth cycle as follows: for Cowan I: 14.5 ± 0.4 (in TSB) / 9.2 ± 0.7 (in PA supernatant + TSB); for 6850: 14.3 ± 0.8 / 10.6 ± 1.7; for JE2: 14.6 ± 0.5 / 13.5 ± 0.6. Thus, our experimental evolution involved at least 140 - 220 bacterial generations (assuming no evolutionary improvements in growth). Following experimental evolution, we plated all evolved populations on 1.2% TSB agar and randomly picked five clones per population for further characterization. All selected clones were first cultured overnight in TSB and then frozen at -80 °C by mixing 50% of culture with 50% of a sterile 85% glycerol solution.

Growth of evolved populations and clones

We tested whether the 42 evolved populations and the selected 210 clones showed improved growth performance relative to the ancestors in the two conditions of our experimental evolution (30% PA supernatant + 70% TSB and 100% TSB). We exposed all populations and clones to the condition they had evolved in, but also to the alternate condition they had not evolved in. For this growth screening, we followed the exact same protocol as the one described above for the supernatant assay.

Staphyloxanthin (STX) quantification

For the subsequent phenotypic and genotypic assays, we used a total of 150 clones from 30 populations (5 clones per population). Sample size was reduced to meet the sequencing contingent of this project. In a first assay, we tested whether evolved clones changed staphyloxanthin (STX) production compared to the respective ancestor. We quantified this SA

636 pigment based on a previously published protocol (Antonic et al. 2013). Briefly, we first
637 collected 1 ml from each culture of all evolved clones and ancestors (grown overnight in TSB)
638 and resuspended washed pellets in 400 µl methanol. We incubated the samples for 10 min at
639 55 °C, pelleted cells by centrifugation and collected the supernatant containing the STX.
640 Absorbance of the crude extract was measured in duplicates at λ = 465 nm using a plate reader
641 (Tecan Infinite M200 pro). We blank-corrected STX values and expressed them first, relative
642 to the blank-corrected OD_{600} of the respective clone and second, relative to the respective STX
643 value of the ancestor.
644
645 **Hydrogen peroxide (H_2O_2) survival assay**
646 To determine whether evolved clones are better at surviving under oxidative stress conditions,
647 we performed a hydrogen peroxide (H_2O_2) survival assay, which we adapted from a previously
648 published protocol (Hall et al. 2017). In short, we subjected cultures of all evolved clones and
649 ancestors (grown overnight in TSB) to either 1.5% H_2O_2 or 0.8% NaCl (as control) for one hour
650 at 37 °C. Subsequently, we plated dilutions on 1.2% TSB agar, incubated plates overnight at
651 37 °C and enumerated colony forming units (CFUs) on the next day. We then calculated the
652 percentage survival for each clone as the CFUs from the H_2O_2 treatment divided by the CFUs
653 from the control treatment multiplied by 100.
654
655 **Small colony variant (SCV) detection and quantification**
656 To determine whether evolved clones express SCV phenotypes, we plated cultures of all
657 evolved clones on 1.2% TSB agar, incubated plates overnight at 37 °C, and then classified the
658 colonies with an area smaller than 20% of the ancestral colony size as SCV. To estimate the
659 prevalence of SCVs at the population level, we also serially diluted and plated aliquots of every
660 evolved population on 1.2% TSB agar and assessed the percentage of SCVs per population
661 after incubation of plates overnight at 37 °C.
662
663

664 **Hemolysis assay**

665 The ancestral strains of 6850 and JE2 are known for their ability to lyse red blood cells
666 (hemolysis), whereas Cowan I is unable to do so. To determine whether evolved clones of
667 6850 and JE2 show different hemolysis patterns compared to their ancestors, we plated
668 cultures of all evolved clones and ancestors (grown overnight in TSB) on COS plates (columbia
669 agar + 5% sheep blood, Biomérieux, Petit-Lancy, Switzerland). COS plates were incubated
670 overnight at 37 °C. On the next day, we qualitatively assessed the hemolysis pattern of each
671 clone according to three discrete categories: ancestral-like hemolysis (wild-type like), reduced
672 hemolysis, (almost) absent hemolysis (examples depicted in Figure 6c). In addition, we also
673 plated all evolved populations on COS plates to assess the frequency of the three hemolysis
674 phenotypes within populations.

675

676 **Genome sequencing**

677 To identify genetic changes in evolved clones relative to their ancestors, we extracted the
678 genomic DNA of all 150 phenotypically characterized clones and the three ancestral SA
679 strains. We used the Maxwell RSC Cultured Cells DNA Kit (Promega, Dübendorf, Switzerland)
680 together with the Maxwell RSC 48 instrument (Promega) following the manufacturer's protocol.
681 To lyse the gram-positive SA cells, we added lysostaphin (L7386, Sigma-Aldrich) to the
682 samples (final concentration of 25 µg per 400 µl sample). DNA concentrations were quantified
683 using the QuantiFluor dsDNA sample kit (Promega). Library preparation was performed with
684 100 ng of DNA input using the TruSeq DNA Nano kit (Illumina, San Diego, USA) according to
685 the manufacturers' instructions. The libraries were quantified using the Tapestation (Agilent
686 Technologies, Santa Clara, USA) and qPCR (Roche, Rotkreuz, Switzerland) and equimolarly
687 pooled. Finally, the libraries were sequenced 150 bp paired-end on the NovaSeq6000 system
688 (Illumina, San Diego, USA). The samples had an estimated coverage of 100x for the evolved
689 clones and 200x for the three SA ancestors.

690 The quality of the raw sequencing data was assessed using FastQC (version 0.11.9)
691 (https://www.bioinformatics.babraham.ac.uk/projects/fastqc/) and a contamination check was

performed using Fastqscreen (version 0.14.1). Subsequently, the raw reads were preprocessed using Trimmomatic (Bolger, Lohse, and Usadel 2014) with the following settings: trimmString="ILLUMINACLIP: adapters.fa:1:30:10 LEADING:15 TRAILING:15 SLIDINGWINDOW:5:30 AVGQUAL:32 MINLEN:80". All the reads that passed the trimming and quality filtering steps were analyzed using Snippy (https://github.com/tseemann/snippy) (v4.5.2) with default parameters. For the ancestral strains 6850 and JE2, the reads were aligned to the published reference genomes (GenBank accession Nr. CP006706.1 and NZ_CP020619.1, respectively). Variants that were present in the ancestor compared to the published reference genome were removed and only those variants that occurred during experimental evolution were kept. Finally, we used SnpEff version 4.3t (built 2017-11-24 10:18) (https://pcingola.github.io/SnpEff/) to predict variant effects. For Cowan I, no suitable reference genome was available, and we thus performed a *de novo* assembly with SPAdes (v3.12.0) and annotation with Prodigal (v2.6.3) using the reads from our ancestor, and then directly called the variants as in the other two strains for the evolved clones relative to the *de novo* assembled ancestral genome. Note that one clone had to be discarded after library preparation due to poor DNA quality.

Statistical analysis

All statistical analyses were performed with R Studio version 3.6.3. We used general linear models wherever possible and consulted Q-Q plots and the Shapiro-Wilk test to examine whether residuals were normally distributed. The basic linear model that we used was an analysis of variance (ANOVA) in which we put the response variable in relation to the manipulated factors, which are (i) the SA strain background (Cowan I, 6850, JE2), (ii) the experimental conditions (presence/absence of PA supernatant or PQS concentration), and (iii) the interaction between the two. We used variants of this model for statistical analysis of all growth data, STX production, and survival in the presence of H_2O_2 as response variables. Non-significant interactions were removed from the models. If data was not normally distributed (as

719 for the survival data), we $\log_{10}(x+1)$-transformed all values for statistical analysis and scaled
720 them back to the respective ancestor for plotting.

721 We performed one sample t-tests to test whether STX production and survival in the
722 presence of H_2O_2 in evolved clones was significantly different from the expected ancestral
723 value. The false discovery rate method was used to correct p-values whenever necessary. For
724 frequency comparisons between hemolysis categories for 6850 and JE2 clones evolved in the
725 two media, we performed Fisher's exact tests. The principle component analysis (PCA) was
726 performed on clonal phenotypes using the *vegan* package in R. We tested for inference using
727 permutational multivariate analysis of variance (PERMANOVA).

Competing interests

The authors declare that no competing interests exist.

Author Contributions

S.N. and R.K. designed research, S.N. performed research, L.P. and J.G. analyzed the genome sequencing data, S.N. and R.K. analyzed all other datasets and wrote the paper with inputs from L.P. and J.G. All authors approved the manuscript prior to submission.

Funding

This project has received funding from the European Research Council under the European Union's Horizon 2020 research and innovation program (grant agreement no. 681295) to RK, from the Swiss National Science Foundation (31003A_182499) to RK, and from the University of Zürich Teaching Fund (2019_12 / Fostering OMICS research through research- based teaching and learning) to LP and JG.

Acknowledgements

We thank Markus Huemer and Annelies Zinkernagel (University Hospital of Zürich) for providing *S. aureus* strains, the Eberl group (University of Zürich) for providing the *P. aeruginosa ΔpqsA* strain, Jay Tracy for helping with DNA extraction, Maria Domenica Moccia for performing the whole genome sequencing, Giancarlo Russo for bioinformatic analysis, and Alexandre Figueiredo for comments about the manuscript. Illustration for Supplementary Figure 4 was created using BioRender (www.biorender.com).

Data availability statement

All raw data sets will be deposited in an online repository upon the acceptance of the manuscript.

References

Abdalla, Maher Y., Traci Hoke, Javier Seravalli, Barbara L. Switzer, Melissa Bavitz, Jill D. Fliege, Peter J. Murphy, and Bradley E. Britigan. 2017. “Pseudomonas Quinolone Signal Induces Oxidative Stress and Inhibits Heme Oxygenase-1 Expression in Lung Epithelial Cells.” *Infection and Immunity* 85 (9): 1–14. https://doi.org/doi: 10.1128/IAI.00176-17.

Antonic, Vlado, Alexander Stojadinovic, Binxue Zhang, Mina J. Izadjoo, and Mohammad Alavi. 2013. “Pseudomonas Aeruginosa Induces Pigment Production and Enhances Virulence in a White Phenotypic Variant of Staphylococcus Aureus.” *Infection and Drug Resistance* 6: 175–86. https://doi.org/10.2147/IDR.S49039.

Biswas, Lalitha, Raja Biswas, Martin Schlag, Ralph Bertram, and Friedrich Götz. 2009. “Small-Colony Variant Selection as a Survival Strategy for Staphylococcus Aureus in the Presence of Pseudomonas Aeruginosa.” *Applied and Environmental Microbiology* 75 (21): 6910–12. https://doi.org/10.1128/AEM.01211-09.

Bolger, Anthony M., Marc Lohse, and Bjoern Usadel. 2014. “Trimmomatic: A Flexible Trimmer for Illumina Sequence Data.” *Bioinformatics* 30 (15): 2114–20. https://doi.org/10.1093/bioinformatics/btu170.

Bredenbruch, Florian, Robert Geffers, Manfred Nimtz, Jan Buer, and Susanne Häussler. 2006. “The Pseudomonas Aeruginosa Quinolone Signal (PQS) Has an Iron-Chelating Activity.” *Environmental Microbiology* 8 (8): 1318–29. https://doi.org/10.1111/j.1462-2920.2006.01025.x.

Brogden, Kim A, Janet M Guthmiller, and Christopher E Taylor. 2005. “Human Polymicrobial Infections.” *Lancet* 365 (9455): 253–55. https://doi.org/https://doi.org/10.1016/S0140-6736(05)17745-9.

Burnside, Kellie, Annalisa Lembo, Melissa de los Reyes, Anton Iliuk, Nguyen Thao BinhTran, James E. Connelly, Wan Jung Lin, et al. 2010. “Regulation of Hemolysin Expression and Virulence of Staphylococcus Aureus by a Serine/Threonine Kinase and Phosphatase.” *PLoS ONE* 5 (6). https://doi.org/10.1371/journal.pone.0011071.

783 Camus, Laura, Paul Briaud, François Vandenesch, and Karen Moreau. 2021. “How Bacterial
784 Adaptation to Cystic Fibrosis Environment Shapes Interactions Between Pseudomonas
785 Aeruginosa and Staphylococcus Aureus.” *Frontiers in Microbiology* 12 (March): 1–16.
786 https://doi.org/10.3389/fmicb.2021.617784.
787 Cheung, Gordon Y.C., Justin S. Bae, and Michael Otto. 2021. “Pathogenicity and Virulence
788 of Staphylococcus Aureus.” *Virulence* 12 (1): 547–69.
789 https://doi.org/10.1080/21505594.2021.1878688.
790 Clauditz, Alexandra, Alexandra Resch, Karsten Peter Wieland, Andreas Peschel, and
791 Friedrich Götz. 2006. “Staphyloxanthin Plays a Role in the Fitness of Staphylococcus
792 Aureus and Its Ability to Cope with Oxidative Stress.” *Infection and Immunity* 74 (8):
793 4950–53. https://doi.org/10.1128/IAI.00204-06.
794 Corrigan, Rebecca M., James C. Abbott, Heike Burhenne, Volkhard Kaever, and Angelika
795 Gründling. 2011. “C-Di-AMP Is a New Second Messenger in Staphylococcus Aureus
796 with a Role in Controlling Cell Size and Envelope Stress.” *PLoS Pathogens* 7 (9).
797 https://doi.org/10.1371/journal.ppat.1002217.
798 Dalton, Trevor, Scot E. Dowd, Randall D. Wolcott, Yan Sun, Chase Watters, John A.
799 Griswold, and Kendra P. Rumbaugh. 2011. “An in Vivo Polymicrobial Biofilm Wound
800 Infection Model to Study Interspecies Interactions.” *PLoS ONE* 6 (11).
801 https://doi.org/10.1371/journal.pone.0027317.
802 Deurenberg, Ruud H., and Ellen E. Stobberingh. 2008. “The Evolution of Staphylococcus
803 Aureus.” *Infection, Genetics and Evolution* 8 (6): 747–63.
804 https://doi.org/10.1016/j.meegid.2008.07.007.
805 Diep, Binh An, Steven R. Gill, Richard F. Chang, Tiffany HaiVan Phan, Jason H. Chen,
806 Matthew G. Davidson, Felice Lin, et al. 2006. “Complete Genome Sequence of
807 USA300, an Epidemic Clone of Community-Acquired Meticillin-Resistant
808 Staphylococcus Aureus.” *Lancet* 367 (4): 731–39. https://doi.org/DOI: 10.1016/S0140-
809 6736(06)68231-7.
810 Diggle, Stephen P., Sandra Matthijs, Victoria J. Wright, Matthew P. Fletcher, Siri Ram

811 Chhabra, Iain L. Lamont, Xiaole Kong, et al. 2007. “The Pseudomonas Aeruginosa 4-
812 Quinolone Signal Molecules HHQ and PQS Play Multifunctional Roles in Quorum
813 Sensing and Iron Entrapment.” *Chemistry and Biology* 14 (1): 87–96.
814 https://doi.org/10.1016/j.chembiol.2006.11.014.
815 Dowd, Scot E., Yan Sun, Patrick R. Secor, Daniel D. Rhoads, Benjamin M. Wolcott, Garth A.
816 James, and Randall D. Wolcott. 2008. “Survey of Bacterial Diversity in Chronic Wounds
817 Using Pyrosequencing, DGGE, and Full Ribosome Shotgun Sequencing.” *BMC*
818 *Microbiology* 8 (43): 1–15. https://doi.org/10.1186/1471-2180-8-43.
819 Dubern, Jean Frédéric, and Stephen P. Diggle. 2008. “Quorum Sensing by 2-Alkyl-4-
820 Quinolones in Pseudomonas Aeruginosa and Other Bacterial Species.” *Molecular*
821 *BioSystems* 4 (9): 882–88. https://doi.org/10.1039/b803796p.
822 Fazli, Mustafa, Thomas Bjarnsholt, Klaus Kirketerp-Møller, Bo Jørgensen, Anders Schou
823 Andersen, Karen A. Krogfelt, Michael Givskov, and Tim Tolker-Nielsen. 2009.
824 “Nonrandom Distribution of Pseudomonas Aeruginosa and Staphylococcus Aureus in
825 Chronic Wounds.” *Journal of Clinical Microbiology* 47 (12): 4084–89.
826 https://doi.org/10.1128/JCM.01395-09.
827 Filkins, Laura M., Jyoti A. Graber, Daniel G. Olson, Emily L. Dolben, Lee R. Lynd, Sabin
828 Bhuju, and George A. O’Toole. 2015. “Coculture of Staphylococcus Aureus with
829 Pseudomonas Aeruginosa Drives S. Aureus towards Fermentative Metabolism and
830 Reduced Viability in a Cystic Fibrosis Model.” *Journal of Bacteriology* 197 (14): 2252–
831 64. https://doi.org/10.1128/JB.00059-15.
832 Fuchs, Stephan, Henry Mehlan, Jörg Bernhardt, André Hennig, Stephan Michalik, Kristin
833 Surmann, Jan Pané-Farré, et al. 2018. “AureoWiki - The Repository of the
834 Staphylococcus Aureus Research and Annotation Community.” *International Journal of*
835 *Medical Microbiology* 308 (6): 558–68. https://doi.org/10.1016/j.ijmm.2017.11.011.
836 Gangell, Catherine, Samantha Gard, Tonia Douglas, Judy Park, Nicholas De Klerk, Tony
837 Keil, Siobhain Brennan, Sarath Ranganathan, Roy Robins-Browne, and Peter D. Sly.
838 2011. “Inflammatory Responses to Individual Microorganisms in the Lungs of Children

839 with Cystic Fibrosis." *Clinical Infectious Diseases* 53 (5): 425–32.
840 https://doi.org/10.1093/cid/cir399.
841 Gjødsbøl, Kristine, Jens Jørgen Christensen, Tonny Karlsmark, Bo Jørgensen, Bjarke M.
842 Klein, and Karen A. Krogfelt. 2006. "Multiple Bacterial Species Reside in Chronic
843 Wounds: A Longitudinal Study." *International Wound Journal* 3 (3).
844 https://doi.org/10.1111/j.1742-481X.2006.00159.x.
845 Hall, Jeffrey W, Junshu Yang, Haiyong Guo, and Yinduo Ji. 2017. "The Staphylococcus
846 Aureus AirSR Two- Component System Mediates Reactive Oxygen Species Resistance
847 via Transcriptional Regulation of Staphyloxanthin Production." *Infection and Immunity*
848 85 (2): 1–12. https://doi.org/DOI: 10.1128/IAI.00838-16.
849 Harrison, Freya, Jon Paul, Ruth C. Massey, and Angus Buckling. 2008. "Interspecific
850 Competition and Siderophore-Mediated Cooperation in Pseudomonas Aeruginosa."
851 *ISME Journal* 2 (1): 49–55. https://doi.org/10.1038/ismej.2007.96.
852 Hendricks, Kelly J., Tim A. Burd, Jeffrey O. Anglen, Andrew W. Simpson, Gordon D.
853 Christensen, and Barry J. Gainor. 2001. "Synergy Between Staphylococcus Aureus and
854 Pseudomonas Aeruginosa in a Rat Model of Complex Orthopaedic Wounds." *The*
855 *Journal of Bone & Joint Surgery* 83 (6). https://doi.org/DOI:10.2106/00004623-
856 200106000-00006.
857 Hoffman, Lucas R., Eric Déziel, David A. D'Argenio, François Lépine, Julia Emerson, Sharon
858 McNamara, Ronald L. Gibson, Bonnie W. Ramsey, and Samuel I. Miller. 2006.
859 "Selection for Staphylococcus Aureus Small-Colony Variants Due to Growth in the
860 Presence of Pseudomonas Aeruginosa." *Proceedings of the National Academy of*
861 *Sciences of the United States of America* 103 (52): 19890–95.
862 https://doi.org/10.1073/pnas.0606756104.
863 Hotterbeekx, An, Samir Kumar-Singh, Herman Goossens, and Surbhi Malhotra-Kumar.
864 2017. "In Vivo and In Vitro Interactions between Pseudomonas Aeruginosa and
865 Staphylococcus Spp." *Frontiers in Cellular and Infection Microbiology* 7 (APR): 1–13.
866 https://doi.org/10.3389/fcimb.2017.00106.

867 Hubert, Dominique, Hélène Réglier-Poupet, Isabelle Sermet-Gaudelus, Agnès Ferroni,
868 Muriel Le Bourgeois, Pierre Régis Burgel, Raphaël Serreau, Daniel Dusser, Claire
869 Poyart, and Joël Coste. 2013. “Association between Staphylococcus Aureus Alone or
870 Combined with Pseudomonas Aeruginosa and the Clinical Condition of Patients with
871 Cystic Fibrosis.” *Journal of Cystic Fibrosis* 12 (5): 497–503.
872 https://doi.org/10.1016/j.jcf.2012.12.003.
873 Huemer, Markus, Srikanth Mairpady Shambat, Silvio D Brugger, and Annelies S Zinkernagel.
874 2020. “Antibiotic Resistance and Persistence—Implications for Human Health and
875 Treatment Perspectives.” *EMBO Reports* 21 (12): 1–24.
876 https://doi.org/10.15252/embr.202051034.
877 Ibberson, Carolyn B., and Marvin Whiteley. 2020. “The Social Life of Microbes in Chronic
878 Infection.” *Current Opinion in Microbiology* 53: 44–50.
879 https://doi.org/10.1016/j.mib.2020.02.003.
880 Jorge, Luciana Souza, Patrícia Silva Fucuta, Maria Gabriele L., Marcelo Arruda Nakazone,
881 Juliana Arruda de, Alceu Gomes Chueire, and Mauro José Costa. 2018. “Outcomes and
882 Risk Factors for Polymicrobial Posttraumatic Osteomyelitis.” *Journal of Bone and Joint*
883 *Infection* 3 (1): 20–26. https://doi.org/10.7150/jbji.22566.
884 Kahl, Barbara C, Karsten Becker, and Bettina Löffler. 2016. “Clinical Significance and
885 Pathogenesis of Staphylococcal Small Colony Variants in Persistent Infections.”
886 *American Society for Microbiology* 29 (2): 401–27. https://doi.org/10.1128/CMR.00069-
887 15.
888 Kessler, E., M. Safrin, J. C. Olson, and D. E. Ohman. 1993. “Secreted LasA of Pseudomonas
889 Aeruginosa Is a Staphylolytic Protease.” *Journal of Biological Chemistry* 268 (10):
890 7503–8.
891 Leimer, Nadja, Carole Rachmühl, Miguel Palheiros Marques, Anna Sophie Bahlmann,
892 Alexandra Furrer, Fritz Eichenseher, Kati Seidl, et al. 2016. “Nonstable Staphylococcus
893 Aureus Small-Colony Variants Are Induced by Low PH and Sensitized to Antimicrobial
894 Therapy by Phagolysosomal Alkalinization.” *Journal of Infectious Diseases* 213 (2):

305–13. https://doi.org/10.1093/infdis/jiv388.

Lensmire, Joshua M, Jack P Dodson, Brian Y Hsueh, Michael R Wischer, Phillip C Delekta, John C Shook, Elizabeth N Ottosen, Paige J Kies, Janani Ravi, and Neal D. Hammer. 2020. “The Staphylococcus Aureus Cystine Transporters TcyABC and TcyP Facilitate Nutrient Sulfur Acquisition during Infection.” *Infection and Immunity* 88 (3). https://doi.org/https://doi.org/10.1128/IAI.00690-19.

Lim, Nigel C.S., Dawn K.A. Lim, and Manotosh Ray. 2013. “Polymicrobial versus Monomicrobial Keratitis: A Retrospective Comparative Study.” *Eye and Contact Lens* 39 (5): 348–54. https://doi.org/10.1097/ICL.0b013e3182a3024e.

Limoli, Dominique H., and Lucas R. Hoffman. 2019. “Help, Hinder, Hide and Harm: What Can We Learn from the Interactions between Pseudomonas Aeruginosa and Staphylococcus Aureus during Respiratory Infections.” *Thorax* 74 (7): 684–92. https://doi.org/10.1136/thoraxjnl-2018-212616.

Lin, Jinshui, Juanli Cheng, Yao Wang, and Xihui Shen. 2018. “The Pseudomonas Quinolone Signal (PQS): Not Just for Quorum Sensing Anymore.” *Frontiers in Cellular and Infection Microbiology* 8 (JUL): 1–9. https://doi.org/10.3389/fcimb.2018.00230.

Maliniak, Maret L., Arlene A. Stecenko, and Nael A. McCarty. 2016. “A Longitudinal Analysis of Chronic MRSA and Pseudomonas Aeruginosa Co-Infection in Cystic Fibrosis: A Single-Center Study.” *Journal of Cystic Fibrosis* 15 (3): 350–56. https://doi.org/10.1016/j.jcf.2015.10.014.

Mashburn, Lauren M., Amy M. Jett, Darrin R. Akins, and Marvin Whiteley. 2005. “Staphylococcus Aureus Serves as an Iron Source for Pseudomonas Aeruginosa during in Vivo Coculture.” *Journal of Bacteriology* 187 (2): 554–66. https://doi.org/10.1128/JB.187.2.554-566.2005.

Nguyen, Angela T., and Amanda G. Oglesby-Sherrouse. 2016. “Interactions between Pseudomonas Aeruginosa and Staphylococcus Aureus during Co-Cultivations and Polymicrobial Infections.” *Applied Microbiology and Biotechnology* 100 (14): 6141–48. https://doi.org/10.1007/s00253-016-7596-3.

923 Niggli, Selina, and Rolf Kümmerli. 2020. “Strain Background, Species Frequency, and
924 Environmental Conditions Are Important in Determining Pseudomonas Aeruginosa and
925 Staphylococcus Aureus Population Dynamics and Species Coexistence.” *Applied and*
926 *Environmental Microbiology* 86 (18): 1–14. https://doi.org/DOI: 10.1128/AEM.00962-20.
927 Noto, Michael J., William J. Burns, William N. Beavers, and Eric P. Skaar. 2017.
928 “Mechanisms of Pyocyanin Toxicity and Genetic Determinants of Resistance in
929 Staphylococcus Aureus.” *Journal of Bacteriology* 199 (17): 1–13.
930 https://doi.org/10.1128/JB.00221-17.
931 Orazi, Giulia, and George A. O’Toole. 2017. “Pseudomonas Aeruginosa Alters
932 Staphylococcus Aureus Sensitivity to Vancomycin in a Biofilm Model of Cystic Fibrosis
933 Infection.” *MBio* 8 (4): 1–17. https://doi.org/10.1128/mBio.00873-17.
934 Pammi, Mohan, Danni Zhong, Yvette Johnson, Paula Revell, and James Versalovic. 2014.
935 “Polymicrobial Bloodstream Infections in the Neonatal Intensive Care Unit Are
936 Associated with Increased Mortality: A Case-Control Study.” *BMC Infectious Diseases*
937 14 (1): 1–8. https://doi.org/10.1186/1471-2334-14-390.
938 Pastar, Irena, Aron G. Nusbaum, Joel Gil, Shailee B. Patel, Juan Chen, Jose Valdes, Olivera
939 Stojadinovic, Lisa R. Plano, Marjana Tomic-Canic, and Stephen C. Davis. 2013.
940 “Interactions of Methicillin Resistant Staphylococcus Aureus USA300 and
941 Pseudomonas Aeruginosa in Polymicrobial Wound Infection.” *PLoS ONE* 8 (2): 1–11.
942 https://doi.org/10.1371/journal.pone.0056846.
943 Peters, Brian M., Mary Ann Jabra-Rizk, Graeme A. O’May, J. William Costerton, and Mark E.
944 Shirtliff. 2012. “Polymicrobial Interactions: Impact on Pathogenesis and Human
945 Disease.” *Clinical Microbiology Reviews* 25 (1): 193–213.
946 https://doi.org/10.1128/CMR.00013-11.
947 Phalak, Poonam, Jin Chen, Ross P. Carlson, and Michael A. Henson. 2016. “Metabolic
948 Modeling of a Chronic Wound Biofilm Consortium Predicts Spatial Partitioning of
949 Bacterial Species.” *BMC Systems Biology* 10 (1): 1–20. https://doi.org/10.1186/s12918-
950 016-0334-8.

951 Pollitt, Eric J.G., Stuart A. West, Shanika A. Crusz, Maxwell N. Burton-Chellew, and Stephen
952 P. Diggle. 2014. “Cooperation, Quorum Sensing, and Evolution of Virulence in
953 Staphylococcus Aureus.” *Infection and Immunity* 82 (3): 1045–51.
954 https://doi.org/10.1128/IAI.01216-13.
955 Popat, Roman, Freya Harrison, Ana C. da Silva, Scott A.S. Easton, Luke McNally, Paul
956 Williams, and Stephen P. Diggle. 2017. “Environmental Modification via a Quorum
957 Sensing Molecule Influences the Social Landscape of Siderophore Production.”
958 *Proceedings of the Royal Society B: Biological Sciences* 284 (1852).
959 https://doi.org/10.1098/rspb.2017.0200.
960 Ramos, Ana F., David F. Woods, Rachel Shanahan, Rafael Cano, Gerard P. McGlacken,
961 Claudia Serra, Fergal O’Gara, and F. Jerry Reen. 2020. “A Structure-Function Analysis
962 of Interspecies Antagonism by the 2-Heptyl-4-Alkyl-Quinolone Signal Molecule from
963 Pseudomonas Aeruginosa.” *Microbiology* 166 (2): 169–79.
964 https://doi.org/10.1099/mic.0.000876.
965 Rezzoagli, Chiara, Elisa T. Granato, and Rolf Kümmerli. 2020. “Harnessing Bacterial
966 Interactions to Manage Infections: A Review on the Opportunistic Pathogen
967 Pseudomonas Aeruginosa as a Case Example.” *Journal of Medical Microbiology* 69 (2):
968 147–61. https://doi.org/10.1099/jmm.0.001134.
969 Schieber, Michael, and Navdeep S. Chandel. 2014. “ROS Function in Redox Signaling and
970 Oxidative Stress.” *Current Biology* 24 (10): R453–62.
971 https://doi.org/10.1016/j.cub.2014.03.034.
972 Serra, Raffaele, Raffaele Grande, Lucia Butrico, Alessio Rossi, Ugo Francesco Settimio,
973 Benedetto Caroleo, Bruno Amato, Luca Gallelli, and Stefano De Franciscis. 2015.
974 “Chronic Wound Infections: The Role of Pseudomonas Aeruginosa and Staphylococcus
975 Aureus.” *Expert Review of Anti-Infective Therapy* 13 (5): 605–13.
976 https://doi.org/10.1586/14787210.2015.1023291.
977 Shopsin, Bo, Alex Drlica-Wagner, Barun Mathema, Rajan P. Adhikari, Barry N. Kreiswirth,
978 and Richard P. Novick. 2008. “Prevalence of Agr Dysfunction among Colonizing

979 Staphylococcus Aureus Strains." *Journal of Infectious Diseases* 198 (8): 1171–74.
980 https://doi.org/10.1086/592051.
981 Soberón-Chávez, Gloria, François Lépine, and Eric Déziel. 2005. "Production of
982 Rhamnolipids by Pseudomonas Aeruginosa." *Applied Microbiology and Biotechnology*
983 68 (6): 718–25. https://doi.org/10.1007/s00253-005-0150-3.
984 Tan, Timothy L., Michael M. Kheir, Dean D. Tan, and Javad Parvizi. 2016. "Polymicrobial
985 Periprosthetic Joint Infections: Outcome of Treatment and Identification of Risk Factors."
986 *The Journal of Bone and Joint Surgery* 98 (24): 2082–88.
987 https://doi.org/10.2106/jbjs.15.01450.
988 Tognon, Mikaël, Thilo Köhler, Bartosz G. Gdaniec, Youai Hao, Joseph S. Lam, Marie
989 Beaume, Alexandre Luscher, Angus Buckling, and Christian Van Delden. 2017. "Co-
990 Evolution with Staphylococcus Aureus Leads to Lipopolysaccharide Alterations in
991 Pseudomonas Aeruginosa." *ISME Journal* 11 (10): 2233–43.
992 https://doi.org/10.1038/ismej.2017.83.
993 Tognon, Mikaël, Thilo Köhler, Alexandre Luscher, and Christian Van Delden. 2019.
994 "Transcriptional Profiling of Pseudomonas Aeruginosa and Staphylococcus Aureus
995 during in Vitro Co-Culture." *BMC Genomics* 20 (1): 1–15.
996 https://doi.org/10.1186/s12864-018-5398-y.
997 Toyofuku, Masanori, Toshiaki Nakajima-Kambe, Hiroo Uchiyama, and Nobuhiko Nomura.
998 2010. "The Effect of a Cell-to-Cell Communication Molecule, Pseudomonas Quinolone
999 Signal (PQS), Produced by P. Aeruginosa on Other Bacterial Species." *Microbes and*
1000 *Environments* 25 (1): 1–7. https://doi.org/10.1264/jsme2.ME09156.
1001 Traber, Katrina E., Elsie Lee, Sarah Benon, Rebecca Corrigan, Mariela Cantera, Bo Shopsin,
1002 and Richard P. Novick. 2008. "Agr Function in Clinical Staphylococcus Aureus Isolates."
1003 *Microbiology* 154 (8): 2265–74. https://doi.org/10.1099/mic.0.2007/011874-0.
1004 Tuchscherr, Lorena, Eva Medina, Muzaffar Hussain, Wolfgang Völker, Vanessa Heitmann,
1005 Silke Niemann, Dirk Holzinger, et al. 2011. "Staphylococcus Aureus Phenotype
1006 Switching: An Effective Bacterial Strategy to Escape Host Immune Response and

1007 Establish a Chronic Infection." *EMBO Molecular Medicine* 3 (3): 129–41.
1008 https://doi.org/10.1002/emmm.201000115.
1009 Xue, Lijun, Yang Yizhi Chen, Zhiyun Yan, Wei Lu, Dong Wan, and Huifeng Zhu. 2019.
1010 "Staphyloxanthin: A Potential Target for Antivirulence Therapy." *Infection and Drug*
1011 *Resistance* 12: 2151–60. https://doi.org/10.2147/IDR.S193649.
1012 Yung, Deborah Bow Yue, Kathleen Jean Sircombe, and Daniel Pletzer. 2021. " Friends or
1013 Enemies? The Complicated Relationship between Pseudomonas Aeruginosa and
1014 Staphylococcus Aureus ." *Molecular Microbiology*, no. October 2020: 1–15.
1015 https://doi.org/10.1111/mmi.14699.
1016 Zeden, Merve S., Orlà Burke, Moya Vallely, Claire Fingleton, and James P. O'Gara. 2021.
1017 "Exploring Amino Acid and Peptide Transporters as Therapeutic Targets to Attenuate
1018 Virulence and Antibiotic Resistance in Staphylococcus Aureus." *PLoS Pathogens*, 1–5.
1019 https://doi.org/10.1371/journal.ppat.1009093.
1020 Zeden, Merve S., Igor Kviatkovski, Christopher F. Schuster, Vinai C. Thomas, Paul D. Fey,
1021 and Angelika Gründling. 2020. "Identification of the Main Glutamine and Glutamate
1022 Transporters in Staphylococcus Aureus and Their Impact on C-Di-AMP Production."
1023 *Molecular Microbiology* 113 (6): 1085–1100. https://doi.org/10.1111/mmi.14479.
1024